

ATM Activation and Its Recruitment to Damaged DNA Require Binding to the C Terminus of Nbs1

Zhongsheng You,¹† Charly Chahwan,²† Julie Bailis,¹ Tony Hunter,^{1*} and Paul Russell^{2*}

Molecular and Cell Biology Laboratory, The Salk Institute for Biological Studies, 10010 North Torrey Pines Road, La Jolla, California 92037,¹ and Department of Molecular Biology, The Scripps Research Institute, 10550 North Torrey Pines Road, La Jolla, California 92037²

Received 25 March 2005/Returned for modification 3 April 2005/Accepted 7 April 2005

ATM has a central role in controlling the cellular responses to DNA damage. It and other phosphoinositide 3-kinase-related kinases (PIKKs) have giant helical HEAT repeat domains in their amino-terminal regions. The functions of these domains in PIKKs are not well understood. ATM activation in response to DNA damage appears to be regulated by the Mre11-Rad50-Nbs1 (MRN) complex, although the exact functional relationship between the MRN complex and ATM is uncertain. Here we show that two pairs of HEAT repeats in fission yeast ATM (Tel1) interact with an FXF/Y motif at the C terminus of Nbs1. This interaction resembles nucleoporin FXFG motif binding to HEAT repeats in importin- β . Budding yeast Nbs1 (Xrs2) appears to have two FXF/Y motifs that interact with Tel1 (ATM). In *Xenopus* egg extracts, the C terminus of Nbs1 recruits ATM to damaged DNA, where it is subsequently autophosphorylated. This interaction is essential for ATM activation. A C-terminal 147-amino-acid fragment of Nbs1 that has the Mre11- and ATM-binding domains can restore ATM activation in an Nbs1-depleted extract. We conclude that an interaction between specific HEAT repeats in ATM and the C-terminal FXF/Y domain of Nbs1 is essential for ATM activation. We propose that conformational changes in the MRN complex that occur upon binding to damaged DNA are transmitted through the FXF/Y-HEAT interface to activate ATM. This interaction also retains active ATM at sites of DNA damage.

All eukaryotic organisms have highly effective mechanisms of repairing DNA damage. These repair systems are essential for maintaining genome integrity. They work in conjunction with checkpoints that monitor DNA damage and control DNA repair, cell cycle progression, and programmed cell death. Central to these checkpoint systems are the protein kinases ATM and ATR (1, 5, 67). ATM is mutated in patients with ataxia-telangiectasia syndrome, a genetic disorder characterized by neurodegeneration, immunodeficiency, premature aging, telomere dysfunction, genetic instability, radiation sensitivity, and cancer (41). The ATR locus is mutated in some patients with Seckel syndrome, a developmental disorder that is also associated with genetic instability (56). Both kinases can be activated in response to different types of DNA damage, although ATM appears to be more specific for double-strand breaks (DSBs), whereas ATR is particularly important in the cellular response to replication fork arrest. ATM and ATR phosphorylate a partially overlapping set of downstream targets that are involved in DNA repair, checkpoint signaling, and apoptosis. These targets include Brca1, Chk1, Chk2, histone H2AX, and p53, all of which have been shown to be important

for maintenance of genome integrity and suppression of tumors (37).

ATM and ATR belong to a larger superfamily of proteins that have a common C-terminal phosphatidylinositol-3'-OH kinase-like kinase (PIKK) domain, which acts as a protein kinase (1, 5, 67). Other well-known members of this family are TORs (targets of rapamycin), which modulate protein translation and transcription, and DNA-PKs (DNA-dependent protein kinases), which are involved in nonhomologous end joining of DNA. All PIKKs are very large proteins (270 to 450 kDa) in which the C-terminal kinase domain accounts for only 5 to 10% of the total sequence. The remainder of these proteins consists mostly of tandem HEAT (huntingtin, elongation factor 3, A subunit of protein phosphatase 2A, and TOR1) repeats (57). A single HEAT repeat unit is a pair of interacting antiparallel helices joined by a flexible "intraunit" loop (2). Adjacent HEAT repeats are linked by a flexible interunit loop. In crystallographically analyzed proteins, HEAT repeat domains form superhelical scaffolding matrices that can engage other molecules (6, 14, 28). One well-characterized interaction involves FXFG motifs in nucleoporins that contact the convex face of a superhelical HEAT repeat structure in importin- β (6).

The analysis of ATM and ATR has been aided by studies of homologs in the budding yeast *Saccharomyces cerevisiae* and the fission yeast *Schizosaccharomyces pombe*. The ATM homolog is known as Tel1 in both yeasts, whereas ATR is known as Mec1 in budding yeast and Rad3 in fission yeast (55). A recent study of budding yeast Tel1 showed that it interacts with the C-terminal region of Xrs2, a subunit of the Mre11-Rad50-Xrs2 complex (50). This protein complex participates in the

* Corresponding author. Mailing address for Paul Russell: Department of Molecular Biology, MB3, The Scripps Research Institute, 10550 North Torrey Pines Road, La Jolla, CA 92037. Phone: (858) 784-8273. Fax: (858) 784-2265. E-mail: prussell@scripps.edu. Mailing address for Tony Hunter: Molecular and Cell Biology Laboratory, The Salk Institute for Biological Studies, 10010 North Torrey Pines Road, La Jolla, CA 92037. Phone: (858) 453-4100. Fax: (858) 457-4765. E-mail: hunter@salk.edu.

† These authors contributed equally to this work.

TABLE 1. *S. pombe* strains used in this study

Strain	Genotype ^a	Source or reference
PR109	Wild type	Lab stock
CC3223	<i>nbs1::kanMX6</i>	11
LLD3260	<i>h⁻ leu1-32::2YFP-crb2⁺ -leu1⁺ ura4-D18 crb2-D2::ura4⁺</i>	22
LLD3341	<i>his3-D1 crb2::ura4⁺ -2YFP-crb2⁺ -leu1⁺ tel1-D1::kanMX4 rad3::ura4⁺</i>	51
CC3575	<i>nbs1⁺ -TAP:kanMX6</i>	This study
CC3576	<i>nbs1ΔC60-TAP:kanMX6</i>	This study
CC3577	<i>nbs1-9-TAP:kanMX6</i>	This study
CC3578	<i>nbs1-10-TAP:kanMX6</i>	This study
CC3579	<i>kanMX6:nmt1-TAP-tel1⁺ nbs1⁺ -13myc:kanMX6</i>	This study
CC3580	<i>kanMX6:nmt1-TAP-tel1⁺ nbs1-9-13myc:kanMX6</i>	This study
CC3581	<i>kanMX6:nmt1-TAP-tel1⁺ nbs1-10-13myc:kanMX6</i>	This study
CC3582	<i>rad3::ura4⁺ nbs1⁺ -TAP:kanMX6 mrc1⁺ -TAP:kanMX6</i>	This study
CC3583	<i>rad3::ura4⁺ nbs1 ΔC60-TAP:kanMX6 mrc1⁺ -TAP:kanMX6</i>	This study
CC3584	<i>rad3::ura4⁺ nbs1-9-TAP:kanMX6 mrc1⁺ -TAP:kanMX6</i>	This study
CC3585	<i>rad3::ura4⁺ nbs1-10-TAP:kanMX6 mrc1⁺ -TAP:kanMX6</i>	This study
CC3586	<i>rad3::ura4⁺ tel1-D2:Leu2 mrc1⁺ -TAP:kanMX6</i>	This study
CC3587	<i>ade6⁻ his3-D1 crb2::ura4⁺ -2YFP-crb2⁺ -leu1⁺ rad3::ura4⁺ nbs1⁺ -TAP:kanMX6</i>	This study
CC3588	<i>ade6⁻ his3-D1 crb2::ura4⁺ -2YFP-crb2⁺ -leu1⁺ rad3::ura4⁺ nbs1ΔC60-TAP:kanMX6</i>	This study
CC3589	<i>ade6⁻ his3-D1 crb2::ura4⁺ -2YFP-crb2⁺ -leu1⁺ rad3::ura4⁺ nbs1-9-TAP:kanMX6</i>	This study
CC3590	<i>ade6⁻ his3-D1 crb2::ura4⁺ -2YFP-crb2⁺ -leu1⁺ rad3::ura4⁺ nbs1-10-TAP:kanMX6</i>	This study

^a All strains are *h⁻ leu1-32 ura4-D18*.

early recognition and processing of DSBs (44, 58). The Mre11 and Rad50 subunits are highly conserved through evolution, whereas Xrs2, which is known as Nbs1 in most other species, is poorly conserved at the primary sequence level. Biochemical and structural studies have shown that the Mre11-Rad50-Nbs1 (MRN) complex has DNA-binding, nuclease, unwinding, and end-bridging activities (15). The MRN complex is required for efficient homologous recombination and nonhomologous end joining, it participates in telomere maintenance, and it is involved in intra-S and G₂-M checkpoint signaling (18, 30). The MRN complex is required for the efficient recruitment of ATM/Tel1 to sites of DNA damage and for the efficient phosphorylation of ATM/Tel1 substrates at these sites (9, 10, 36, 38, 44, 50).

The exact function of the MRN complex in controlling ATM activation is not yet fully understood. The MRN complex is essential in vertebrates (20); hence, many of the relevant studies have used cells from patients with Nijmegen breakage syndrome (NBS) or ataxia-telangiectasia-like disorder (ATLD) that express reduced amounts of truncated but not fully defective forms of Nbs1 or Mre11, respectively. These studies have typically assayed ATM activation by detecting autophosphorylation on serine-1981 (S1981). ATM autophosphorylation has often been found to be defective in NBS and ATLD cells (9, 10, 19, 36, 38, 48, 73), although in some situations only weak impairment in ATM autophosphorylation was observed in NBS cells (10, 38). For example, a recent study found that ATM autophosphorylation was defective in NBS cells assayed 15 min after exposure to 3 Gy of ionizing radiation, but at 60 min there was no defect in ATM autophosphorylation (10). These findings were interpreted to indicate that the role of Nbs1 in ATM activation was likely to be indirect, perhaps serving to transport Mre11-Rad50 into the nucleus, where it can process DSBs to facilitate rapid activation of ATM. Other experimental approaches have used adenovirus infection to trigger Mre11 degradation (9) or have depleted Mre11 from a *Xenopus* egg extract and assayed phosphorylation of ATM

substrates (16). These studies supported the conclusion that the MRN complex is required for ATM activation, although this interpretation has been disputed (5, 37). An alternative model has been suggested in which ATM senses changes in chromatin structure caused by DNA damage through an MRN-independent mechanism, leading to autophosphorylation of ATM dimers, dissociation of these dimers into active monomers, and subsequent MRN-dependent recruitment of active ATM to sites of DNA damage (4, 5). It has also been proposed that by recruiting active ATM to sites of DNA damage, the MRN complex may stabilize or enhance ATM autophosphorylation by an unknown mechanism (5).

Here we describe studies carried out with Nbs1 and ATM/Tel1 proteins from fission yeast, humans, and *Xenopus*. These studies define an FxY motif in the carboxyl (C) tail of Nbs1 that interacts with a subset of HEAT repeats in ATM/Tel1. In *Xenopus* egg extracts, this interaction is essential for recruitment of ATM to sites of DNA damage and for ATM activation. These findings support a model in which recruitment of ATM to sites of DNA damage and activation of ATM are coupled through binding to the C terminus of Nbs1. We discuss these findings in light of recent contradictory evidence that ATM activation does not require an interaction with Nbs1 (23).

MATERIALS AND METHODS

Yeast strains. Truncated and mutant tagged *nbs1* and *tel1* fission yeast variants (listed in Table 1) were generated by PCR cassette mutagenesis as previously described (3). Oligonucleotide primers used in this study are available upon request.

Microscopy. Duplicate 10-ml cultures of each strain were collected, and one set was irradiated with 100 gray in a 3.3-Gy/min ¹³⁷Cs irradiator. Irradiated and unirradiated cells were collected by centrifugation. For yellow fluorescent protein (YFP)-Crb2 fluorescence microscopy, images were photographed at eight Z-sections at 0.5-μm increments and projected into one image as previously described (22). These studies used a DeltaVision optical sectioning microscope model 283 equipped with a Photometrix CH350L charge-coupled device camera. For analysis of phospho-histone H2A, spread nuclei were prepared as described previously (32). Briefly, cells were spheroplasted in phosphate-buffered saline (PBS) buffer with 1 mg/ml zymolyase 20T (Seikagaku) and lysing enzymes

(Sigma), then washed in MES-Sorbitol buffer (0.1 M 2-N-morpholino ethane sulfonic acid, 1 M sorbitol, 1 mM EDTA, 0.5 mM MgCl₂, pH 6.4), resuspended in 100 μ l MES-Sorbitol buffer and 360 μ l 4% paraformaldehyde, and fixed onto poly-L-lysine-coated slides. Slides were heat fixed before blocking in PBS containing 5% calf serum and incubating with anti-phospho-histone H2AX antibodies (polyclonal rabbit antibodies from Upstate Biotechnology) at 1:50 in block solution. Phospho-histone-H2AX was detected after incubation with chicken anti-rabbit Alexa Fluor 488 antibodies (Molecular Probes) at 1:500. DNA was visualized with DAPI (4',6'-diamidino-2-phenylindole). For each experiment, 100 spread nuclei were counted per strain for unirradiated and irradiated samples.

DNA damage sensitivity assays, immunoprecipitation analysis in yeast, and yeast two-hybrid analysis. Damage sensitivity assays were performed as previously described (11). For immunoprecipitation analysis, whole-cell extracts were prepared from exponentially growing cells in minimal medium lacking thiamine and processed as previously described with the exception that 0.05% Triton X-100 was substituted for 0.1% NP-40 in the lysis buffer (52). Gal4-based Matchmaker Two-Hybrid System 3 (Clontech) was used for the yeast two-hybrid assay according to the manufacturer's instructions. *S. cerevisiae* strain AH109 was used as the reporter strain. The indicated proteins were fused to the GAL4 activation domain in vector pGADT7 or the GAL4 DNA-binding domain in pGBKT7 and expressed in AH109. The interactions were judged by plating on selective minimal medium plates (SC): the control plate SC-TL (minimal medium lacking tryptophan and leucine) was used to select for cotransformation of plasmids, and the high-stringency SC-HTLA (lacking histidine, tryptophan, leucine, and adenine) was used to identify positive interactions. In the analysis of the HEAT repeats (HR) of Tel1, the constructs were as follows: HR 1-12, amino acids 1 to 716; HR 13-24, 751 to 1295; HR 25-36, 1300 to 1851; HR 37-49, 1852 to 2427; kinase domain, 2430 to 2812; HR 13-14, 751 to 833; HR 15-16, 864 to 940; HR 17-18, 941 to 1032; HR 19-20, 1034 to 1110; HR 21-22, 1111 to 1200; and HR 23-24, 1201 to 1295.

Xenopus methods. The *Xenopus* Nbs1 sequence was assembled from two expressed sequence tag sequences (BF426540 and CA988284) that have significant homology with human Nbs1 and confirmed by multiple other expressed sequence tag sequences. Together, the overlapping cDNA clones defined a complete open reading frame of 763 amino acids. Nucleotide sequences of *Xenopus* Nbs1 can be accessed in GenBank (accession no. AY999019). Mutations in GST-C50m1 (E749N and D750N) and GST-C50m2 (F752E and F754E) were generated using a QuikChange site-directed mutagenesis kit (Stratagene). Interphase egg extracts were prepared essentially as described previously (75). The Nbs1 antibodies were raised in rabbits using a His-green fluorescent protein (GFP) fusion protein containing the C-terminal 147 amino acids of *Xenopus* Nbs1. Antibodies against different regions of C-terminal Nbs1 (e.g., C-terminal 50 amino acids) were affinity purified from the anti-C147 serum using the indicated glutathione S-transferase (GST) fusion proteins. The purified antibodies did not recognize His-GFP or GST (data not shown). ATM antibodies were raised in rabbits using a GST fusion protein containing the C-terminal 300 amino acids of *Xenopus* ATM and affinity purified using a His-GFP fusion protein containing the same ATM region. The Mre11 antibody was purchased from Oncogene Research Products (Cat. no. PC388). The anti-C50, anti-C147, ATM, and Mre11 antibodies are described below. The pS1981-ATM and S1981-ATM antibodies were purchased from Rockland Immunochemicals (catalog no. 600-401-400 and 600-401-398). The Ku70 antibody was purchased from Covance (Cat. no. MMS-263R). GST and His-GFP fusion proteins were expressed in *Escherichia coli* strain BL21(DE3) and affinity purified using glutathione agarose resin (Amersham Biosciences) and Talon metal affinity resin (BD Biosciences). Quantification of the immunoblots was done with an Odyssey infrared imaging system from LI-COR Biosciences.

For immunodepletion in *Xenopus* egg extracts, 20 μ l of protein A agarose beads coupled with 15 μ g of purified anti-C147 Nbs1 antibody or nonspecific rabbit immunoglobulin G (IgG) was incubated with 50 μ l of extract for 1 h at 4°C. Beads were then removed by low-speed centrifugation, and the supernatants were taken as depleted extract. For immunoprecipitation in the *Xenopus* egg extracts, 2 μ g of antibodies was incubated with 50 μ l of extract diluted with equal volume of egg lysis buffer for 1 h at 4°C followed by the addition of 30 μ l of protein A agarose beads. After another hour of incubation, beads were washed with buffer 1 (10 mM HEPES, pH 7.8, 100 mM NaCl, 50 mM KCl, 2.5 mM MgCl₂, 250 mM sucrose) or buffer 2 (20 mM HEPES, pH 7.4, 150 mM NaCl, 0.1% NP-40). For GST pull-down, 30 μ l of glutathione beads was incubated with 20 μ g of GST or GST fusion proteins for 1 h at 4°C. After being washed with PBS once, beads were incubated with 40 μ l of extract for 2 h at 4°C. Beads were then isolated and washed four times with buffer (20 mM HEPES, 150 mM NaCl, 0.1% NP-40, pH 7.4). For DNA binding assay, a one-end-biotinylated 2-kb DNA

fragment was generated by PCR using pBluescript as a template and a 5'-biotinylated primer. Subsequently, 5 μ l of magnetic avidin beads (DynaL Biotech) coupled with 40 ng of biotinylated DNA fragment was incubated with 20 μ l of egg extracts at room temperature for the indicated times. After incubation, beads were isolated and washed twice with 200 μ l of egg lysis buffer. DNA-associated proteins were detected by Western blotting.

RESULTS

Conserved Tel1/ATM-binding motifs in *S. pombe* and human Nbs1. The C-terminal 162 amino acids of *S. cerevisiae* Xrs2 are required for its binding to Tel1 (50). The Xrs2/Nbs1 family of proteins is extremely divergent, particularly in the region C-terminal to the conserved NFKXF motif that is required for binding to Mre11 (21, 70); thus, it was unclear whether the Tel1 interaction domain in *S. cerevisiae* Xrs2 is conserved in other species (50). We addressed this question by analysis of fission yeast Nbs1 and Tel1 in a yeast two-hybrid assay. This analysis showed that full-length Nbs1 had a robust interaction with full-length Tel1 (Fig. 1A). Nbs1 also interacted strongly with full-length Rad32 (Fig. 1A), the Mre11 homolog in fission yeast that will hereafter be referred to as Mre11. Mutational studies of the NFKXF motif in Nbs1 showed that it was essential for the yeast two-hybrid interaction with Mre11 but not with Tel1 (Fig. 1B). Truncation of the C-terminal 60 amino acids of Nbs1 (*nbs1- Δ C60*) abolished its interaction with Tel1 while leaving the binding to Mre11 intact (Fig. 1A). Importantly, the C-terminal 50 amino acids of Nbs1 were sufficient for Tel1 binding but did not interact with Mre11 (Fig. 1A and B).

These studies showed that the C-terminal 50 amino acids of Nbs1 contain a Tel1-binding domain that does not overlap with the Mre11-binding domain. These findings suggested that Tel1-binding domains are likely to be conserved between *S. cerevisiae* Xrs2 and *S. pombe* Nbs1. Upon close inspection, we noticed that these proteins shared an FXX motif at their extreme C termini (Fig. 1C). This motif was conserved in other fungi, and it aligned with a highly conserved FXY motif in the C termini of many metazoan Nbs1 proteins (Fig. 1C). We also noticed that the FXX motif in *S. pombe* Nbs1 was preceded by an acidic patch of amino acids (D/E rich) that also appeared to be broadly conserved from fungi to mammals (Fig. 1C).

We investigated the functional significance of these conserved sequences in *S. pombe* Nbs1. We created *nbs1-9* and *nbs1-10* alleles that had mutations in the FXX motif and acidic patch, respectively (Fig. 1C). These mutations were introduced into yeast two-hybrid vectors that expressed full-length Nbs1. Both of these mutations abrogated the two-hybrid interaction with full-length Tel1 (Fig. 1D). To confirm these findings in fission yeast, we replaced the genomic copy of *nbs1*⁺ with the *nbs1-9* or *nbs1-10* alleles and determined whether the mutant proteins coprecipitated with overexpressed Tel1. These studies showed that Tel1 precipitated with wild-type Nbs1 but not with mutant Nbs1 proteins encoded by *nbs1-9* or *nbs1-10* (Fig. 1E). We conclude that the D/E-rich and FXX motifs at the extreme C terminus of *S. pombe* Nbs1 are both essential elements of the Tel1-binding domain.

These studies were extended to human Nbs1 and ATM. Full-length human ATM and Nbs1 displayed a strong interaction in the yeast two-hybrid assay (Fig. 1D). This interaction was almost completely abolished by mutations in the C-termi-

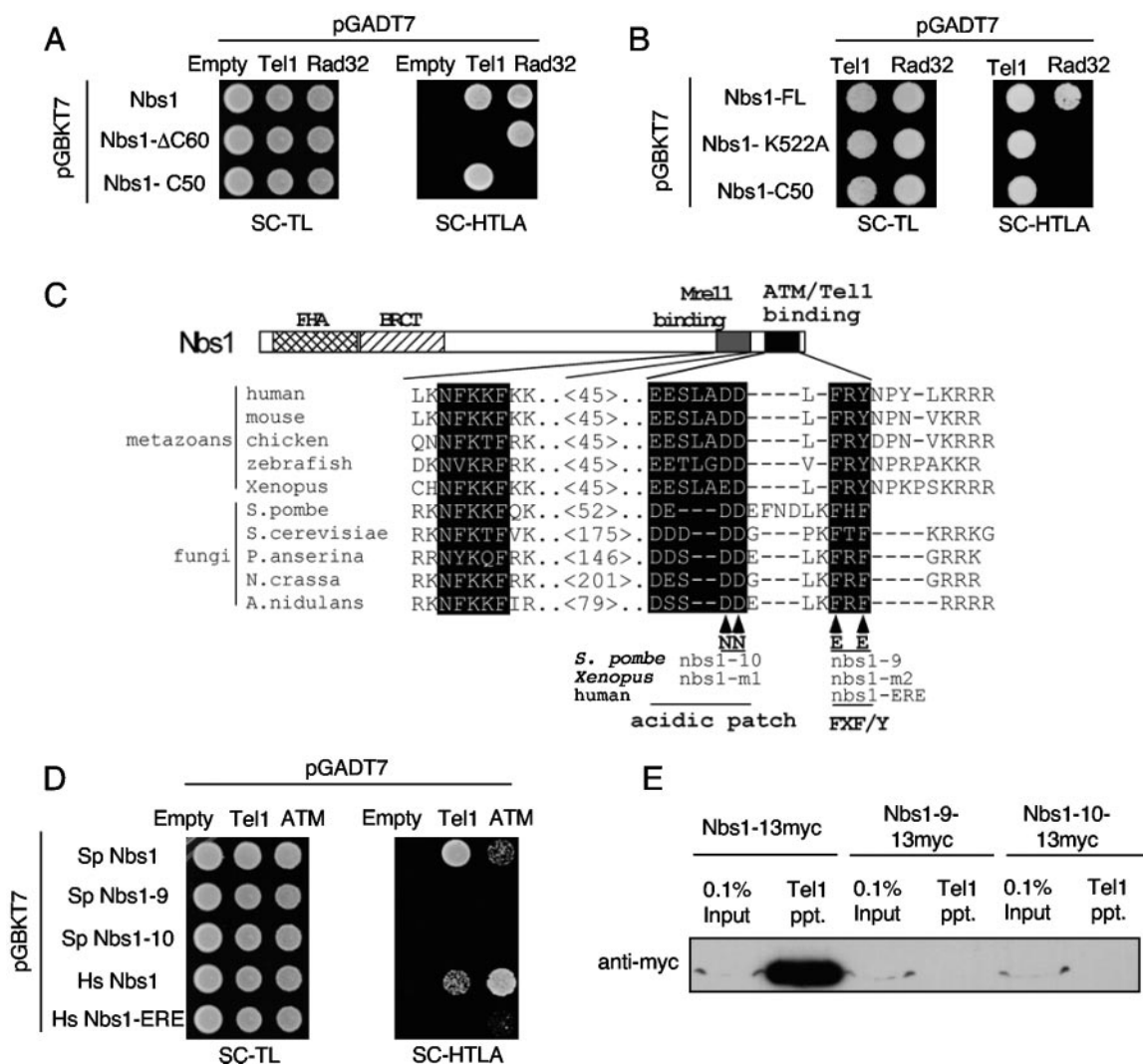


FIG. 1. Conserved motifs at the C terminus of Nbs1 mediate binding to Tel1/ATM. (A) Two-hybrid assays of *S. pombe* Tel1 and Mre11 (Rad32) with full-length Nbs1, a C-terminal truncation of 60 amino acids (Nbs1-ΔC60), or the C-terminal 50 amino acids of Nbs1 (Nbs1-C50). Growth on SC-HTLA medium indicates a positive two-hybrid interaction. (B) A mutation in the Mre11-binding domain of Nbs1 abolishes the two-hybrid interaction with Mre11 without diminishing the interaction between Nbs1 and Tel1. The K522A mutation was created in the Mre11 (Rad32)-binding motif of full-length Nbs1. (C) Alignment of C termini of Nbs1 proteins. The conserved Mre11-binding region, acidic patch, and FXY motif are shown. Mutations created in fission yeast, *Xenopus*, and human Nbs1 proteins are shown. (D) Two-hybrid assays involving *S. pombe* Nbs1 and Tel1, human Nbs1, and ATM. (E) Coprecipitation of Nbs1 with Tel1 in *S. pombe*. TAP-Tel1 expressed from the *mtt1* promoter at the *tel1* genomic locus while 13myc-tagged Nbs1 was expressed from its own promoter at the endogenous locus. TAP-Tel1 was precipitated with protein A Sepharose, and Nbs1-13myc was detected with anti-myc antibodies.

nal FXY motif of human Nbs1 (Fig. 1D). Mutations in the C-terminal acidic patch of human Nbs1 have not been tested. Interestingly, *S. pombe* Nbs1 interacted with human ATM, as did human Nbs1 with *S. pombe* Tel1 (Fig. 1D). Remarkably, these interactions were abolished by mutations in the acidic patch and FXY motif of *S. pombe* Nbs1. Likewise, mutations in the FXY motif of human Nbs1 disrupted the interaction with *S. pombe* Tel1 (Fig. 1D). These findings indicate that the mode of interaction between Tel1/ATM and the C terminus of Nbs1 has been substantially conserved since common ancestors of fission yeast and metazoan organisms diverged over 500 million years ago (31).

The FXY motif and acidic patch in Nbs1 are essential for Tel1 function in fission yeast. A recent study showed that the

C-terminal 89 amino acids of *S. cerevisiae* Xrs2, which contain the highly conserved C-terminal acidic patch and FXY motif (Fig. 1C), are not required for the function of Xrs2 in telomere elongation (71). Xrs2 and Tel1 have fully codependent functions in telomere elongation in *S. cerevisiae* (61); therefore, these observations imply that the C-terminal acidic patch and FXY motif are not required for a productive physical interaction between Tel1 and Xrs2 in *S. cerevisiae*. These findings appeared to conflict with our evidence that the C-terminal acidic patch and FXY motif were essential for the interaction between Nbs1 and Tel1 in *S. pombe*. We therefore performed several assays to assess the functional consequences of mutating the Tel1-binding motifs in Nbs1. To investigate the function of Tel1, we analyzed the C-terminal phosphorylation of

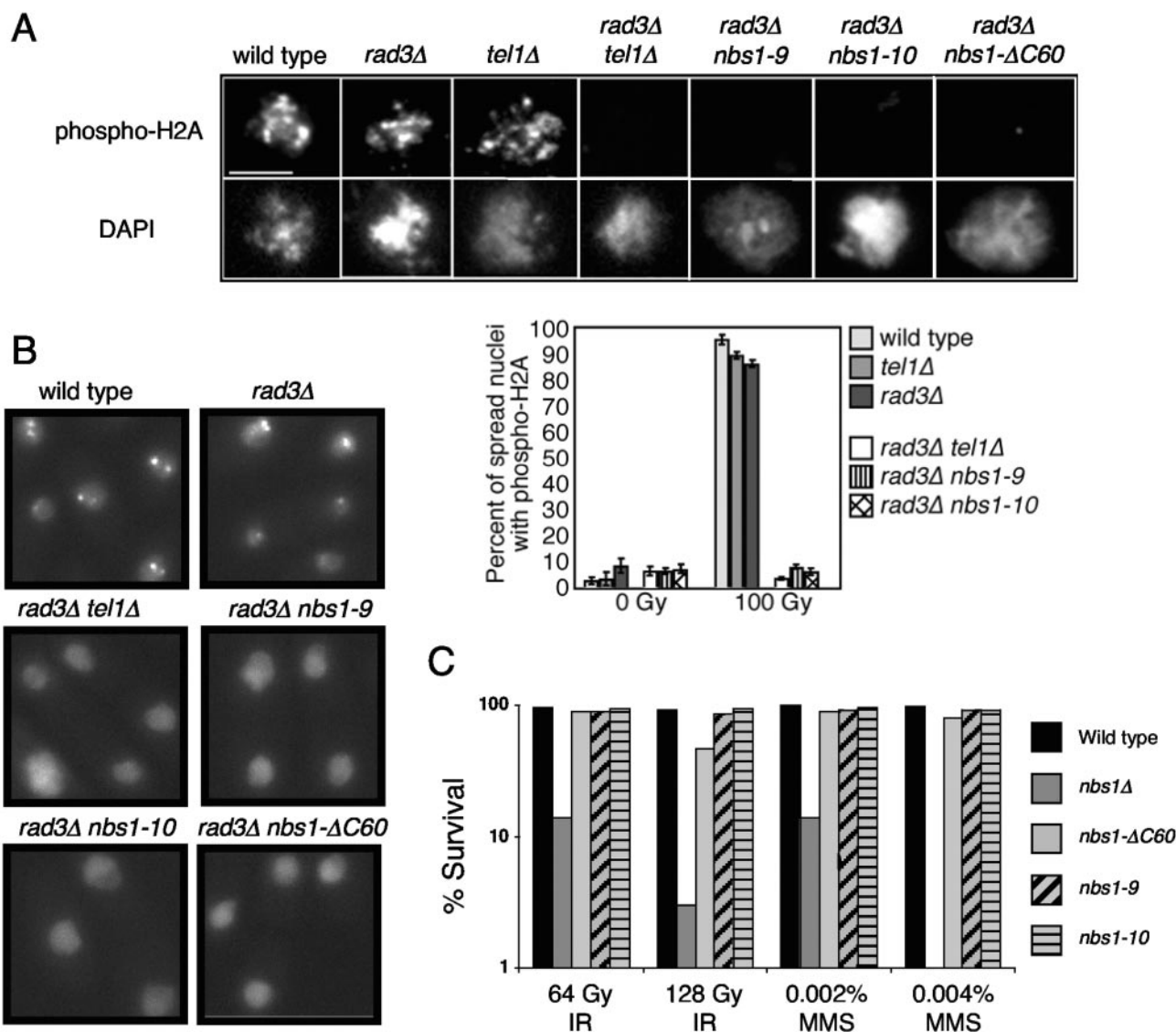


FIG. 2. C-terminal mutations in Nbs1 ablate Tel1 function without impairing the function of Nbs1 in survival of DNA damage. (A) Detection of phospho-histone H2A in chromosome spreads of fission yeast in response to 100 Gy IR. Rad3 and Tel1 both phosphorylate H2A, and therefore *rad3Δ* and *tel1Δ* single mutants have phospho-H2A foci, whereas the *rad3Δ tel1Δ* double mutant has no phospho-H2A foci. In a *rad3Δ* background, mutations in the Tel1-binding motif of Nbs1 abolish induction of phospho-H2A foci. (B) Detection of YFP-Crb2 foci in live cells. Tel1-binding motif mutations in Nbs1 in a *rad3Δ* background abolish induction of YFP-Crb2 foci in response to 30 Gy IR. (C) IR and MMS survival assays show that mutations in the Tel1-binding domain of Nbs1 do not increase the sensitivity to DNA damage.

histone H2A in response to ionizing radiation (IR). This phosphorylation is carried out by Tel1 and Rad3 in fission yeast (51). It is equivalent to the C-terminal phosphorylation of histone H2AX that is catalyzed by ATM and ATR in mammals (25, 60). To specifically assess the activity of Tel1 toward histone H2A, these experiments were performed in a *rad3Δ* background, in which Tel1 function is essential for C-terminal phosphorylation of histone H2A. Histone H2A phosphorylation was monitored in chromosome spreads using a phosphospecific antibody. In a *rad3Δ* background, we found that the C-tail truncation of Nbs1 (*nbs1-ΔC60*), as well as the *nbs1-9* and *nbs1-10* alleles, eliminated the induction of phospho-H2A foci

in response to IR (Fig. 2A). The effect was equivalent to that seen in a *tel1Δ rad3Δ* strain (Fig. 2A).

These findings showed that Tel1 must interact with the C terminus of Nbs1 to be able to phosphorylate histone H2A. We sought to confirm this result by monitoring the formation of IR-induced foci of the checkpoint adaptor protein Crb2. Crb2 is presumed to be the homolog of the mammalian 53BP1 and *S. cerevisiae* Rad9 checkpoint proteins. Crb2 accumulates at DSBs by a mechanism that requires both phospho-H2A and methylation of lysine-20 in histone H4 (22, 51, 64). H4-K20 methylation is not regulated in response to DNA damage, but it is nevertheless essential for effective recruitment or retention

of Crb2 at sites of DNA damage (64). In a *rad3Δ* background, the C-tail truncation of Nbs1 (*nbs1-ΔC60*), as well as the *nbs1-9* and *nbs1-10* alleles, eliminated the induction of Crb2 foci in response to IR (Fig. 2B). The effect was equivalent to deletion of *tel1⁺* in a *rad3Δ* background (Fig. 2B).

These studies demonstrated that the activity of Tel1 toward histone H2A at DSBs requires a functional Tel1-binding domain in Nbs1. In these experiments, we also noticed that the *nbs1-ΔC60*, *nbs1-9*, and *nbs1-10* alleles, combined with the *rad3Δ* mutation, caused a slow-growth and frequent-cell-death phenotype. This phenotype was identical to that observed in *nbs1Δ rad3Δ* and *tel1Δ rad3Δ* strains. The phenotype has been attributed to a defect in telomere maintenance (11, 52, 72). We have not examined telomeres in the strains that combine the Tel1-binding domain mutations of *nbs1* with *rad3Δ*, but their growth properties strongly suggest that the telomere maintenance function of Tel1 requires the conserved acidic patch and FXF/Y motif at the extreme C terminus of Nbs1. These sequences at the extreme C terminus of Xrs2 are not required for telomere elongation in *S. cerevisiae* (71); however, in the Discussion we suggest that Xrs2 may have a second Tel1-binding domain that is not contained within the C-terminal 89-amino-acid truncation analyzed by Tsukamoto et al. (71).

All subunits of the MRN complex, but not Tel1, are vitally important for survival of DNA damage in fission yeast (11, 72). If the C-terminal mutations in the Tel1-binding domain of Nbs1 impaired the general functions of the MRN complex or prevented the MRN complex from recognizing DNA damage, we would expect cells harboring these mutations to be hypersensitive to DNA-damaging agents. Accordingly, we examined whether the mutations in the Tel1-binding domain of Nbs1 impaired the survival of DNA damage. DNA damage was inflicted with IR and the DNA-alkylating agent methyl methanesulfonate. Although *nbs1Δ* mutants were extremely sensitive to these genotoxic agents, the *nbs1-ΔC60*, *nbs1-9*, and *nbs1-10* strains were no more sensitive than the wild type (Fig. 2C). These findings showed that the mutations did not disrupt the function of Nbs1 in DNA repair, despite the fact that these mutations deleted a substantial region of the C terminus of Nbs1 (*nbs1-ΔC60*) or had nonconservative substitutions of the FXF/Y motif (*nbs1-9*). We conclude that the Tel1-binding domain of Nbs1, and specifically the FxF motif and the acidic patch, are not required for function of the MRN complex in the recognition and processing of DNA damage.

Nbs1 interacts with two HEAT repeat regions in Tel1. Having defined the motifs in fission yeast and human Nbs1 that are necessary for binding to Tel1/ATM, we carried out additional two-hybrid assays to map the Nbs1 interaction site(s) in fission yeast Tel1. Tel1 is a 2,812-amino-acid protein that has 49 HEAT repeats (47, 57). Tel1 was divided into five parts for the two-hybrid analyses: HEAT repeats 1 to 12, 13 to 24, 25 to 36, and 37 to 49 and the C-terminal kinase domain (Fig. 3A). This analysis showed that HEAT repeats 13 to 24 interacted strongly with Nbs1, whereas the other regions of Tel1 failed to interact with Nbs1 (Fig. 3B). The 13-24 HEAT repeats were divided pairwise for additional two-hybrid assays. These studies showed that HEAT repeats 17-18 had a strong interaction with Nbs1 and HEAT repeats 21-22 had a somewhat weaker interaction (Fig. 3B). Importantly, these interactions occurred with the C-terminal 50 amino acids of Nbs1 but not with

mutant Nbs1-9 (Fig. 3B). Nbs1-ΔC60 and Nbs1-10 were not tested. We deduce from these findings that HEAT repeats 17-18 and 21-22 each contain an Nbs1-binding site. These interactions specifically require the FXF motif at the C terminus of Nbs1. Interestingly, FFXG motifs in *S. cerevisiae* nucleoporin Nsp1 contact specific HEAT repeats in importin-β (6). These similarities are explored in the Discussion.

Association with the C terminus of Nbs1 is required for the activation of ATM in the *Xenopus* egg extract. We turned to the cell extract system derived from *Xenopus* eggs to carry out a functional analysis of the interaction between ATM and Nbs1. We were particularly interested in determining whether this interaction is required for ATM activation. The *Xenopus* egg extract has been widely used as a model system to study DNA damage signaling pathways (17, 29). These pathways can be activated by addition of linear duplex plasmid DNA. Naked DNA is rapidly assembled into nucleosomes when added to the egg extract (27, 40, 54). We cloned *Xenopus* Nbs1 and made affinity-purified antibodies to the C-terminal 147 amino acids (Fig. 4A). These antibodies detected Nbs1 in ATM complexes immunoprecipitated from *Xenopus* egg extracts (Fig. 5A). This association did not require addition of DNA, but it was disrupted by inclusion of a mild detergent (0.1% NP-40) in the wash buffer (Fig. 5A). These conditions did not disrupt the interaction of Mre11 with Nbs1 (Fig. 5B). Since our studies (see below) and previous investigations have shown that ATM is not autophosphorylated in *Xenopus* egg extracts in the absence of added DNA (65), we deduce that Nbs1 associates with inactive ATM in the absence of DNA damage and that this association is relatively weak or dynamic.

To investigate the interaction between Nbs1 and ATM, we generated GST fusion proteins containing the C-terminal 50 or 147 amino acids of *Xenopus* Nbs1 (GST-C50 or GST-C147, respectively). Both fusion proteins precipitated endogenous ATM from *Xenopus* egg extracts (Fig. 5C), whereas only GST-C147, which contains the Mre11-binding motif, was able to precipitate Mre11 (Fig. 5C). Importantly, the association of GST-C50 with ATM was abolished by mutations that disrupted the acidic patch or the FxY motif (Fig. 5D). These findings provided further support for the functional conservation of the ATM-binding domain at the C terminus of Nbs1.

The *Xenopus* egg extract system was then used to investigate the role of Nbs1 in ATM activation. In human cells, ATM activation correlates with autophosphorylation on serine-1981 (4). We first confirmed that addition of linear double-stranded DNA to *Xenopus* egg extracts led to rapid and potent ATM phosphorylation, as detected with an antibody that recognizes phosphorylated S1981 of human ATM (Fig. 6A). Nbs1, which is a substrate of ATM, was also phosphorylated in response to DSBs (Fig. 6A) (Z. You and T. Hunter, unpublished data). Addition of closed circular plasmid DNA did not stimulate ATM or Nbs1 phosphorylation (Fig. 6A). Interestingly, immunodepletion of Nbs1 from the extract using the anti-C147 antibodies almost completely inhibited ATM autophosphorylation induced in response to linear plasmid DNA (Fig. 6B). In these experiments, quantification of the immunoblots showed that Nbs1 immunodepletion removed ~60% of the Mre11 and 25% of the ATM from the extract. Direct addition of the anti-C147 antibodies to the extract also blocked ATM autophosphorylation (Fig. 6C). These results showed that Nbs1 is

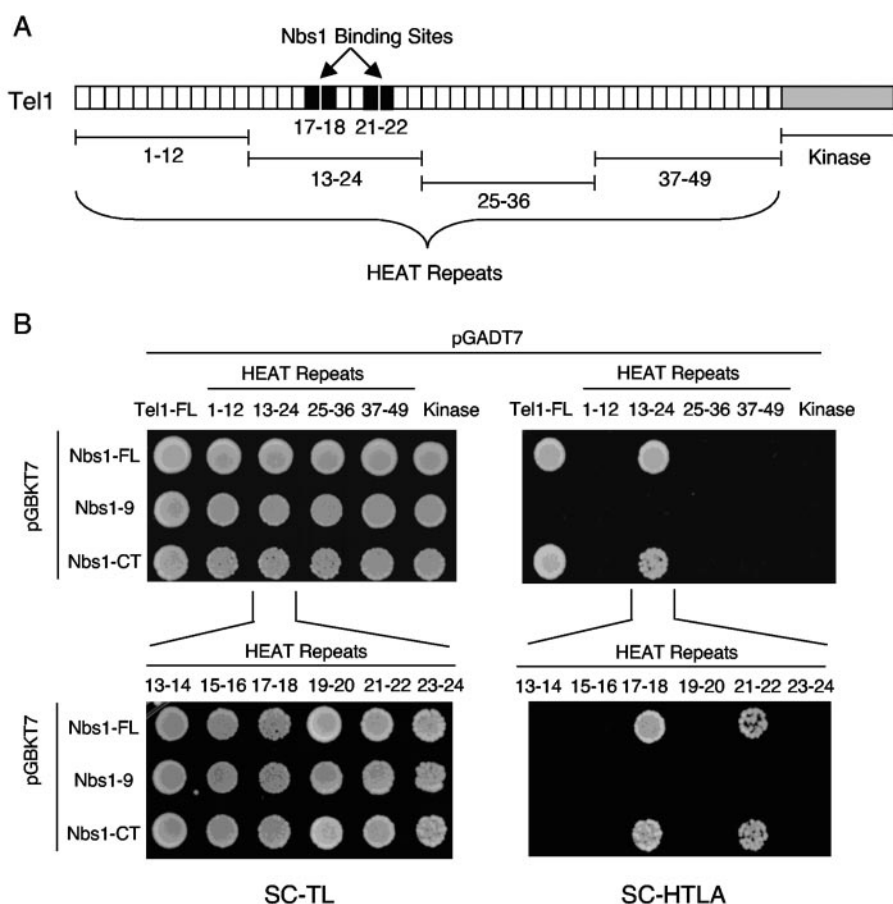


FIG. 3. Nbs1 interacts with specific HEAT repeats 17-18 and 21-22 in Tel1. (A) Schematic of two-hybrid assays with fission yeast Nbs1 and Tel1. (B) Two-hybrid analyses of the regions of Tel1 that interact with Nbs1. The regions of Tel1 that are encoded by the two-hybrid plasmids are described in Materials and Methods. Nbs1-CT indicates the C-terminal 50 amino acids of Nbs1.

required for DSB-induced ATM autophosphorylation in *Xenopus* egg extracts.

Affinity-purified antibodies that recognized the C-terminal 50 amino acids of Nbs1 (anti-C50 antibodies) (Fig. 4B) were also able to inhibit ATM autophosphorylation (Fig. 6C). The inhibitory effects of these antibodies were abrogated by preincubating them with GST-C50 (Fig. 6D). Preincubation with GST-C50 also reversed the inhibitory effects of the anti-C147 antibodies. This result showed that antibodies directed against the C-terminal 50 amino acids of Nbs1 were primarily responsible for the inhibition of ATM activation by the anti-C147 antibodies. Incubating GST-C50 protein alone with the extract did not cause ATM autophosphorylation in the absence of DSBs (data not shown). These data indicated that the C-terminal 50 amino acids of Nbs1 are essential for its role in activating ATM.

As mentioned above, naked plasmid DNA added to *Xenopus* egg extracts is rapidly assembled into chromatin (27, 40, 54). This assembled chromatin appears to be fully functional in a variety of assays—for example, it is efficiently replicated in a semiconservative mechanism (7). However, to confirm that ATM is activated in an Nbs1-dependent manner by damaged chromatin as well as damaged DNA, we carried out experiments with *Xenopus* sperm chromatin. Demembrated sperm

nuclei were incubated with buffer, EcoRI DNA endonuclease (to create DSBs), or heat-inactivated EcoRI. These chromatin preparations were added to *Xenopus* egg extracts. Immunoblotting showed that only the damaged sperm chromatin induced ATM autophosphorylation (Fig. 6E). The damaged chromatin also induced Nbs1 phosphorylation, as observed with addition of linear DNA (Fig. 6A and E).

We repeated these experiments with *Xenopus* egg extracts that were depleted of Nbs1 with the anti-C147 antibodies. Immunoblotting confirmed that Nbs1 was fully depleted from these extracts, whereas most of the ATM and approximately half of the Mre11 protein remained in the extract (Fig. 6F). Damaged chromatin failed to induce ATM autophosphorylation in the Nbs1-depleted samples. In contrast, robust ATM autophosphorylation was detected in the mock-depleted samples. To confirm that direct association of ATM with Nbs1 is required for ATM activation by damaged sperm chromatin, we added anti-C147 and anti-C50 antibodies to the extracts before the addition of damaged sperm chromatin. Both antibodies prevented ATM autophosphorylation induced by damaged chromatin (Fig. 6G). Preincubation of both the anti-C147 and anti-C50 antibodies with GST-C50 reversed their inhibitory effects on ATM autophosphorylation (Fig. 6H). We conclude

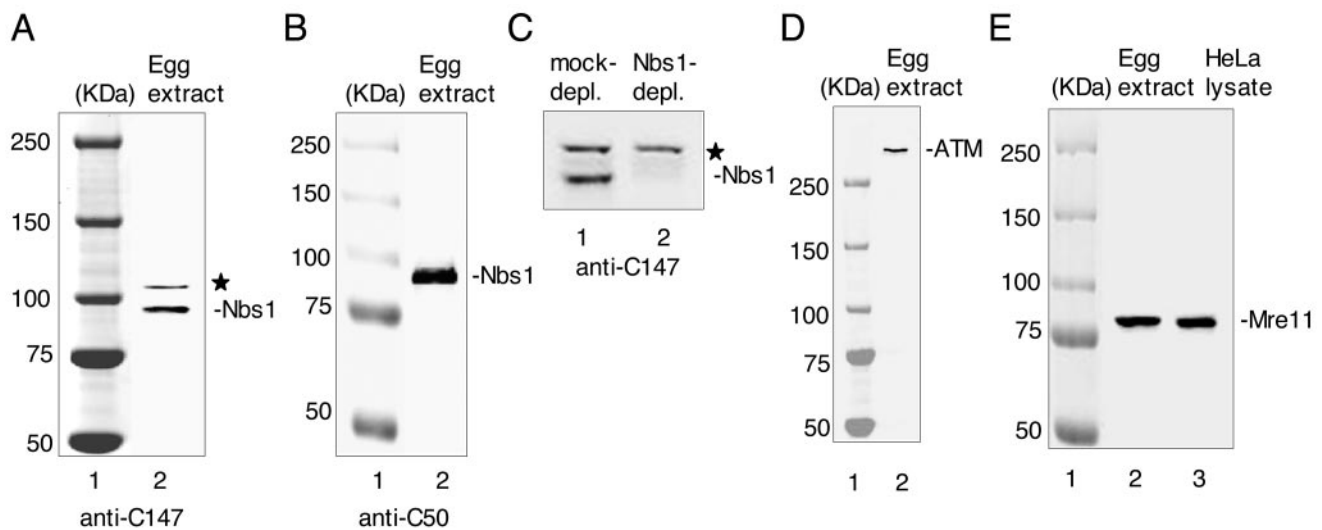


FIG. 4. Characterization of antibodies. (A) Anti-C147 antibodies from rabbits, which were affinity purified with GST-C147 that contained the C-terminal 147 amino acids of *Xenopus* NBS1, were immunoblotted with *Xenopus* egg extract. In addition to Nbs1, a larger-molecular-weight protein (indicated by an asterisk) was also recognized by anti-C147. (B) Anti-C50 antibodies from rabbits, which were affinity purified with GST-C50 that contained the C-terminal 50 amino acids of *Xenopus* NBS1, were immunoblotted with *Xenopus* egg extract. (C) Egg extract was treated with control IgG or anti-C147 to immunodeplete Nbs1. Following depletion, extracts were immunoblotted with anti-C147. Depletion of Nbs1 from the extract using anti-C147 removed Nbs1 but not the larger protein shown in panel A. (D) Anti-ATM antibodies were generated in rabbits using GST-XATMC containing the C-terminal 300 amino acids of *Xenopus* ATM. These antibodies were affinity purified with His-GFP-XATMC and immunoblotted with *Xenopus* egg extract. (E) Shown is an immunoblot of *Xenopus* egg extract and HeLa cell lysate with anti-Mre11 antibodies purchased from Oncogene Research Products.

that Nbs1 is required for the autophosphorylation of ATM that is induced by damaged sperm chromatin.

Recruitment of ATM to DSBs can precede its autophosphorylation. Studies in cells from NBS patients have supported a model in which ATM can be activated in an Nbs1-independent mechanism before it is recruited to sites of DNA damage (4, 5, 38). Our studies with *Xenopus* egg extracts favored an alternative model in which activation of ATM and its recruitment to DSBs are functionally linked through binding to Nbs1. To test this model, we first asked whether ATM is recruited to DSBs in an Nbs1-dependent manner in *Xenopus* egg extracts. Linear 2-kb fragments of DNA were attached to beads and then added to *Xenopus* egg extracts in the presence of anti-C147 antibodies or negative control antibodies. Samples were incubated for 5 min at room temperature before removal of the beads from the extract and detection of associated proteins by immunoblotting. This analysis showed that Nbs1, ATM, and Ku70 (a positive control) were efficiently recruited to the DNA beads in the extract containing control antibodies (Fig. 7A). Immunoblotting with phospho-S1981 antibodies confirmed that ATM was activated in the extract containing control antibodies (Fig. 7A). The anti-C147 antibodies prevented ATM binding to the linear DNA but did not prevent Nbs1 or Ku from interacting with DNA (Fig. 7A). The anti-C147 antibodies also prevented the phosphorylation of Nbs1, which is a substrate of ATM (Fig. 7A). This finding was consistent with the ability of the anti-C147 antibodies to prevent ATM activation (Fig. 6).

The ATM that was bound to DNA was also analyzed with "S1981" antibodies that are specific for the unphosphorylated S1981 epitope. This analysis showed that some of the DNA-

bound ATM was not phosphorylated on S1981 (Fig. 7A). This observation prompted us to analyze samples at 5-minute intervals after addition of DNA beads to the extract. No antibodies were added to the extract in this experiment. We observed that ATM was maximally bound to DNA within 5 min at 25°C (Fig. 7B). The S1981 signal was readily detected at the 5-minute time point, but it returned to a baseline level at subsequent time points. The decrease in the amount of S1981-unphosphorylated ATM was accompanied by a reciprocal increase in the phospho-S1981 signal (Fig. 7B). Quantification of the immunoblot showed that the phospho-S1981 signal increased ~2.5-fold between the 5- and 10-minute samples.

These findings indicated that the interaction of ATM with damaged DNA can precede S1981 phosphorylation. We sought to confirm these findings with damaged sperm chromatin. Consistently, we were able to detect both S1981-unphosphorylated and S1981-phosphorylated ATM binding to damaged chromatin in the extract incubated at room temperature for 5 min. Addition of anti-C147 antibodies inhibited the binding of both unphosphorylated and phosphorylated ATM to damaged chromatin (Fig. 7C). These antibodies also inhibited the phosphorylation of Nbs1 by ATM. We deduce from these findings that ATM can bind damaged chromatin before it undergoes S1981 autophosphorylation. These findings support a mechanism in which activation of ATM and its association with damaged chromatin are coupled through binding to Nbs1.

Mre11- and ATM-binding domains of Nbs1 are sufficient for ATM activation by DSBs. The studies shown in Fig. 6 provided strong evidence that the C-terminal ATM-binding domain of Nbs1 is required for ATM activation in the *Xenopus* egg extract. We extended these studies to identify the domains of

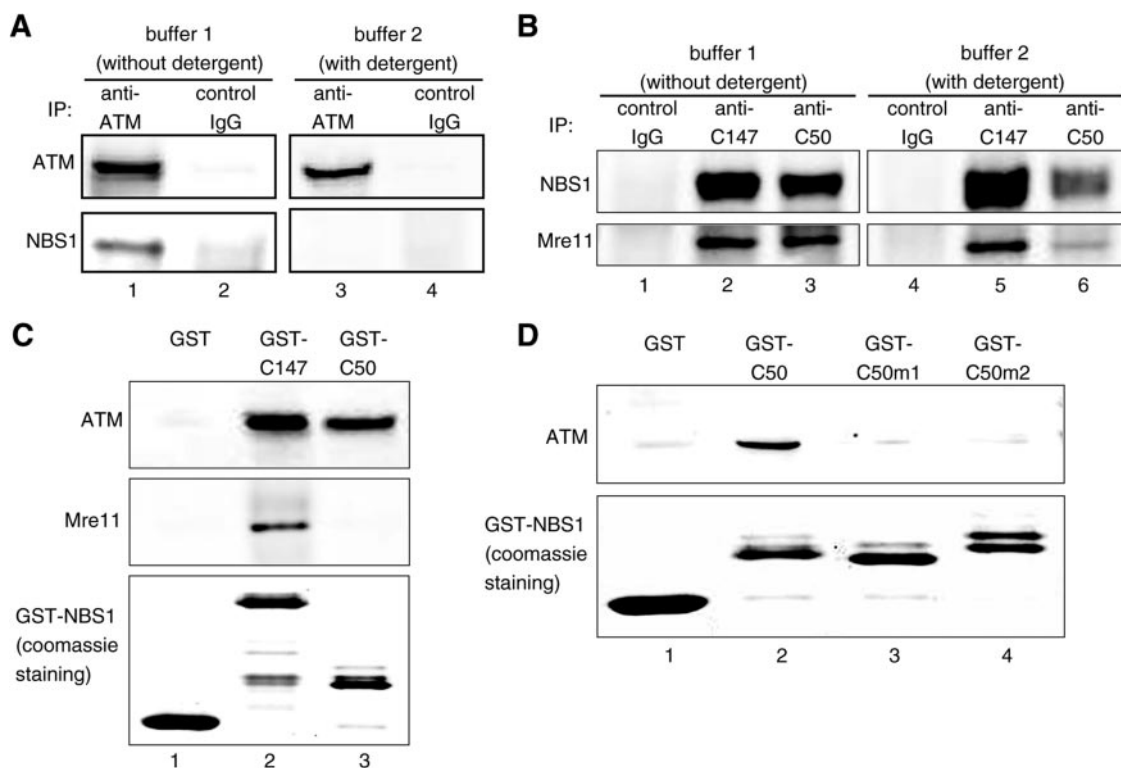


FIG. 5. The acidic patch and FXY motif are essential elements of an ATM-binding domain at the C terminus of *Xenopus* Nbs1. (A) Nbs1 coprecipitates with ATM in *Xenopus* egg extracts. ATM or control immunoprecipitates from *Xenopus* egg extracts were washed four times with buffer 1 (without detergent) or buffer 2 (with 0.1% NP-40), followed by immunoblotting for ATM and Nbs1. (B) Mre11 coprecipitates with Nbs1. Control, anti-C147, and anti-C50 immunoprecipitates of Nbs1 from *Xenopus* egg extracts were washed four times with buffer 1 or buffer 2, as described for panel A, followed by immunoblotting for Nbs1 and Mre11. (C) The C-terminal 50 amino acids of *Xenopus* Nbs1 bind ATM but not Mre11, whereas the C-terminal 147 amino acids of Nbs1 bind to both ATM and Mre11. Glutathione beads coupled with 20 μ g of GST, GST-C147, or GST-C50 recombinant proteins were incubated with 40 μ l of *Xenopus* egg extracts for 2 h at 4°C. The beads were isolated and washed four times with buffer (20 mM HEPES, pH 7.4, 150 mM NaCl, 0.1% NP-40). Proteins associated with the beads were immunoblotted for ATM and Mre11. (D) The acidic patch and FXY motif are essential elements of an ATM-binding domain at the C terminus of *Xenopus* Nbs1. The procedure performed was the same as that described for panel C except that glutathione beads were coupled with 20 μ g of GST, GST-C50, GST-C50m1, or GST-C50m2 recombinant proteins.

Nbs1 that are both necessary and sufficient for ATM activation in response to DSBs. We depleted Nbs1 from the extract and replaced it with bacterially expressed GST fusion proteins containing specific fragments of Nbs1. As shown in Fig. 6B and F, about half of the Mre11 remained after Nbs1 was depleted with the anti-C147 antibodies. To this extract, we added GST fusion proteins containing either the C-terminal 147 amino acids of Nbs1, which contained both the Mre11- and ATM-binding domains, or GST fusion proteins containing the Mre11-binding domain alone (C97) or just the ATM-binding domain (C50). Linearized plasmid DNA was also added to these samples. Remarkably, the C-terminal 147 amino acids of Nbs1 were able to restore ATM autophosphorylation to the Nbs1-depleted extract (Fig. 7D). The GST fusion proteins containing the Mre11-binding domain alone (C97) or the ATM-binding domain alone (C50) were unable to restore ATM autophosphorylation (Fig. 7D). GST-C147 also restored ATM autophosphorylation that was induced by damaged chromatin (Fig. 7E). Furthermore, binding of both unphosphorylated and phosphorylated ATM to immobilized DNA fragments or damaged chromatin was also restored by GST-C147 (Fig. 7F). It should be noted that these incubations were carried out for 2

to 15 min, but even longer incubations (e.g., 30 min) of Nbs1-depleted extracts with damaged DNA or chromatin did not lead to ATM autophosphorylation (Fig. 6F). Therefore, the Nbs1 fragment in GST-C147 is absolutely required for DNA damage-mediated ATM activation and is not just needed for a rapid response to damaged DNA. We conclude from these findings that the Mre11 and ATM-binding domains of Nbs1 define the functions of Nbs1 that are essential for ATM activation.

DISCUSSION

Conserved ATM/Tel1-binding domain at the C terminus of Nbs1. We have shown that a C-terminal ATM/Tel1-binding domain is a conserved feature of Nbs1 proteins in fission yeast, *Xenopus*, and humans. This domain is contained within the C-terminal 50 amino acids of *S. pombe* and *Xenopus* Nbs1. An essential element of this domain is a highly conserved FFX/Y motif that is preceded by an acidic patch of amino acids. Point mutations in these motifs abolish the interaction between Nbs1 and Tel1 in fission yeast and cause a phenotype that is identical to a *tel1* Δ mutant. In the *Xenopus* egg extract, point mutations

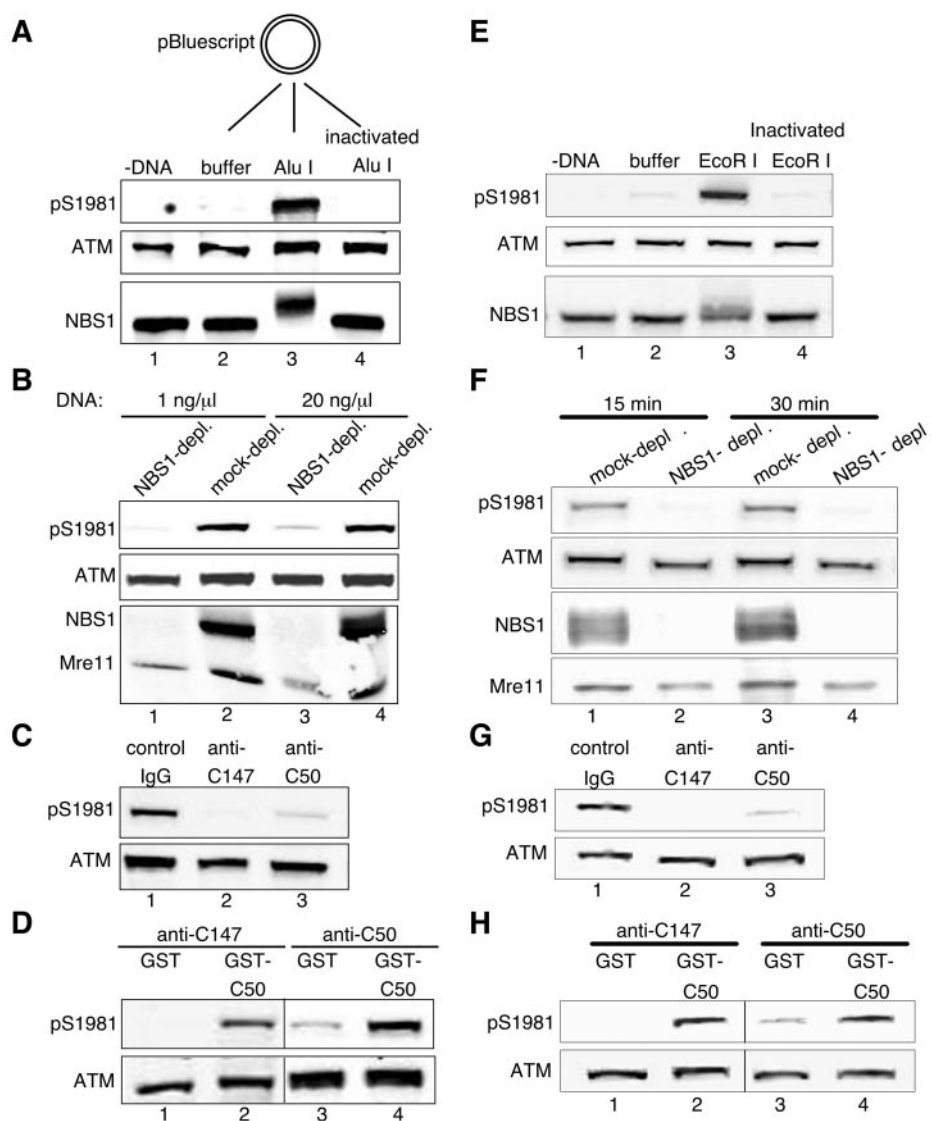


FIG. 6. The C-terminal region of NBS1 is required for ATM activation following addition of linear plasmid DNA or damaged sperm chromatin to the *Xenopus* egg extract. (A) Addition of linear double-stranded DNA induces ATM and NBS1 phosphorylation. *Xenopus* egg extract was incubated for 15 min with no DNA (lane 1) or 1 ng/μl of pBluescript circular plasmid DNA that was incubated with buffer (lane 2), AluI DNA endonuclease (lane 3), or heat-inactivated AluI (lane 4). Extracts were then immunoblotted for pS1981-ATM, total ATM, and NBS1. The gel mobility shift of NBS1 in lane 3 was due to phosphorylation, which is partially dependent on ATM. (B) Immunodepletion of Nbs1 from the extract using the anti-C147 antibodies prevents ATM autophosphorylation induced by linear plasmid DNA. Mock-depleted extracts (lanes 2 and 4) or extracts depleted of NBS1 with anti-C147 antibodies (lanes 1 and 3) were incubated with 1 ng/μl or 20 ng/μl of linearized pBluescript for 15 min. Extracts were immunoblotted for pS1981-ATM, total ATM, and NBS1. Quantification of the immunoblot showed that Nbs1 immunodepletion removed 57% of the Mre11 and 28% of the ATM in the samples that contained 1 ng/μl DNA. Similar values were measured in the 20-ng/μl sample (60% and 24%, respectively). (C) Addition of the anti-C147 and anti-C50 antibodies to the *Xenopus* egg extract blocks ATM autophosphorylation induced by linear plasmid DNA. Extracts containing 300 ng/μl of control IgG or affinity-purified anti-C147 or anti-C50 NBS1 antibodies were incubated with 1 ng/μl of linearized pBluescript for 15 min. Extracts were immunoblotted for pS1981-ATM and total ATM. (D) The inhibitory effects of the anti-C50 and anti-C147 antibodies on ATM autophosphorylation induced by linear plasmid DNA are abrogated by preincubating the antibodies with GST-C50. Anti-C147 or anti-C50 NBS1 antibodies (250 ng/μl) were preincubated with 2 μg/μl of GST or GST-C50 for 20 min at room temperature before being added to extracts containing 1 ng/μl of linearized pBluescript. Following 15 min of incubation, extracts were immunoblotted for pS1981-ATM and total ATM. (E) EcoRI-treated sperm chromatin induces ATM and NBS1 phosphorylation. *Xenopus* egg extract was incubated for 15 min with no DNA (lane 1) or 2,500 demembrated sperm nuclei/μl that were incubated with buffer (lane 2), EcoRI DNA endonuclease (lane 3), or heat-inactivated EcoRI (lane 4). Extracts were then immunoblotted for pS1981-ATM, total ATM, and NBS1. (F) Damaged chromatin fails to induce ATM autophosphorylation in the NBS1-depleted samples. Mock-depleted extracts (lanes 1 and 3) or extracts depleted of NBS1 with anti-C147 antibodies (lanes 2 and 4) were incubated with 2,500 EcoRI-treated demembrated sperm nuclei/μl for 15 min or 30 min. Extracts were immunoblotted for pS1981-ATM, total ATM, and NBS1. Quantification of the immunoblot showed that Nbs1 immunodepletion removed 47% of the Mre11 and 20% of the ATM in the 15-min sample. The corresponding numbers for the 30-min sample were 40% and 21%, respectively. (G) Anti-C50 and anti-C147 antibodies prevent ATM autophosphorylation induced by damaged chromatin. *Xenopus* egg extracts containing 250 ng/μl of control IgG or affinity-purified anti-C147 or anti-C50 NBS1 antibodies were incubated with 2,500 EcoRI-treated demembrated sperm nuclei/μl for 15 min. Extracts were immunoblotted for pS1981-ATM and total ATM. (H) The inhibitory effects of the anti-C50 and anti-C147 antibodies on ATM autophosphorylation induced by damaged chromatin are abrogated by preincubating the antibodies with GST-C50. Anti-C147 or anti-C50 NBS1 antibodies (250 ng/μl) were preincubated with 2 μg/μl of GST or GST-C50 for 20 min at room temperature before being added to extracts containing 2,500 EcoRI-treated demembrated sperm nuclei/μl. Following 15 min of incubation, extracts were immunoblotted for pS1981-ATM and total ATM.

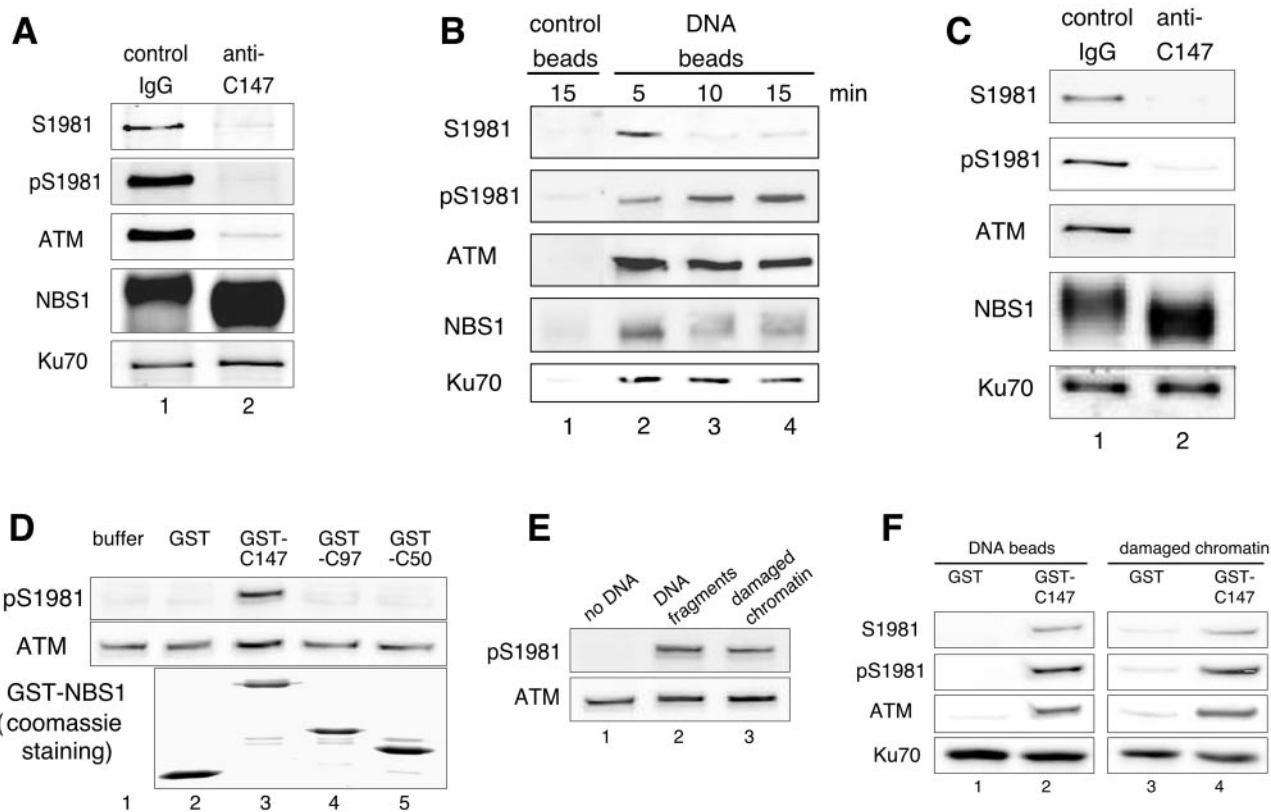


FIG. 7. Recruitment of ATM to DSBs precedes its autophosphorylation, and ATM autophosphorylation in Nbs1-depleted extracts can be restored by the C-terminal 147 amino acids of Nbs1. (A) The anti-C147 antibodies prevent ATM binding to the linear plasmid DNA. Extracts preincubated with 300 ng/ μ l of control IgG or affinity-purified anti-C147 were incubated with magnetic avidin beads coupled with a one-end-biotinylated 2-kb DNA fragment derived from pBluescript. Extracts were incubated with extracts at room temperature for 5 min. Proteins associated with beads were immunoblotted for S1981-ATM (unphosphorylated ATM), pS1981-ATM, total ATM, Ku70, and NBS1. (B) S1981 phosphorylation is not a prerequisite for the interaction of ATM with linear plasmid DNA. Reactions were similar to panel A except samples were not preincubated with antibodies and samples were taken at 5-min intervals following addition of DNA beads. (C) The anti-C147 antibodies prevent ATM binding to damaged sperm chromatin. Extracts preincubated with 250 ng/ μ l of control IgG or affinity-purified anti-C147 were incubated with 2,500 EcoRI-treated demembrated sperm nuclei/ μ l. Extracts were incubated at room temperature for 5 min. Proteins associated with chromatin were immunoblotted for S1981-ATM (unphosphorylated ATM), pS1981-ATM, total ATM, NBS1, and Ku70. (D) A recombinant fragment of Nbs1 that contains the Mre11- and ATM-binding domains restores ATM autophosphorylation to an Nbs1-depleted extract. Anti-C147 antibodies were used to deplete Nbs1 from a *Xenopus* egg extract. Buffer, 100 ng/ μ l GST, GST-C147, GST-C97, or GST-C50 was added to the extract together with linearized plasmid DNA. After 15 min of incubation, extracts were then immunoblotted for pS1981-ATM and total ATM. (E) Linearized plasmid DNA and damaged sperm chromatin induce ATM autophosphorylation in an Nbs1-depleted extract supplemented with a recombinant fragment of Nbs1 that contains the Mre11- and ATM-binding domains. GST-C147 (100 ng/ μ l) was incubated with buffer, 1 ng/ μ l of linearized pBluescript, or 2,500 sperm chromatin treated with EcoRI/ μ l. After 15 min of incubation, extracts were then immunoblotted for pS1981-ATM and total ATM. (F) The C147 fragment of Nbs1 restores ATM binding to linearized plasmid DNA and damaged sperm chromatin in an Nbs1-depleted extract. The Nbs1-depleted extract supplemented with 100 ng/ μ l of GST or GST-C147 was incubated with magnetic avidin beads coupled with one-end-biotinylated 2-kb fragments derived from pBluescript or sperm chromatin treated with EcoRI. After 2 min of incubation, DNA beads and chromatin were isolated and proteins associated with DNA beads or damaged chromatin were immunoblotted for S1981-ATM, pS1981-ATM, total ATM, and Ku70. Similar results were observed after a 10-min incubation except that the S1981-ATM signal was very weak (Z. You and T. Hunter, unpublished data).

in these motifs abolish the ability of the C-terminal 50 amino acids of Nbs1 to precipitate ATM. In yeast two-hybrid assays, mutations in the FXY motif ablate the ability of human Nbs1 to interact with human ATM. Remarkably, therefore, the ability of Nbs1 and Tel1/ATM homologs to interact has been substantially conserved since fission yeast and humans diverged from a common ancestral species over 500 million years ago. We conclude that an FXF/Y motif preceded by an acidic patch of amino acids is a defining feature of Tel1/ATM-binding domains at the C termini of Nbs1 proteins.

Two Tel1-binding domains in Xrs2? The extreme C terminus of *S. cerevisiae* Xrs2 has an FXF motif preceded by an acidic patch of amino acids. These sequences are contained within the C-terminal 15 amino acids of Xrs2. Based on our findings, it is very likely that these sequences are part of a Tel1-binding domain. However, a recent study showed that the C-terminal 89 amino acids of Xrs2 are not essential for its function in telomere maintenance (71). Xrs2 and Tel1 have fully codependent functions in telomere maintenance (61); therefore, it appears that Tel1 function does not require the

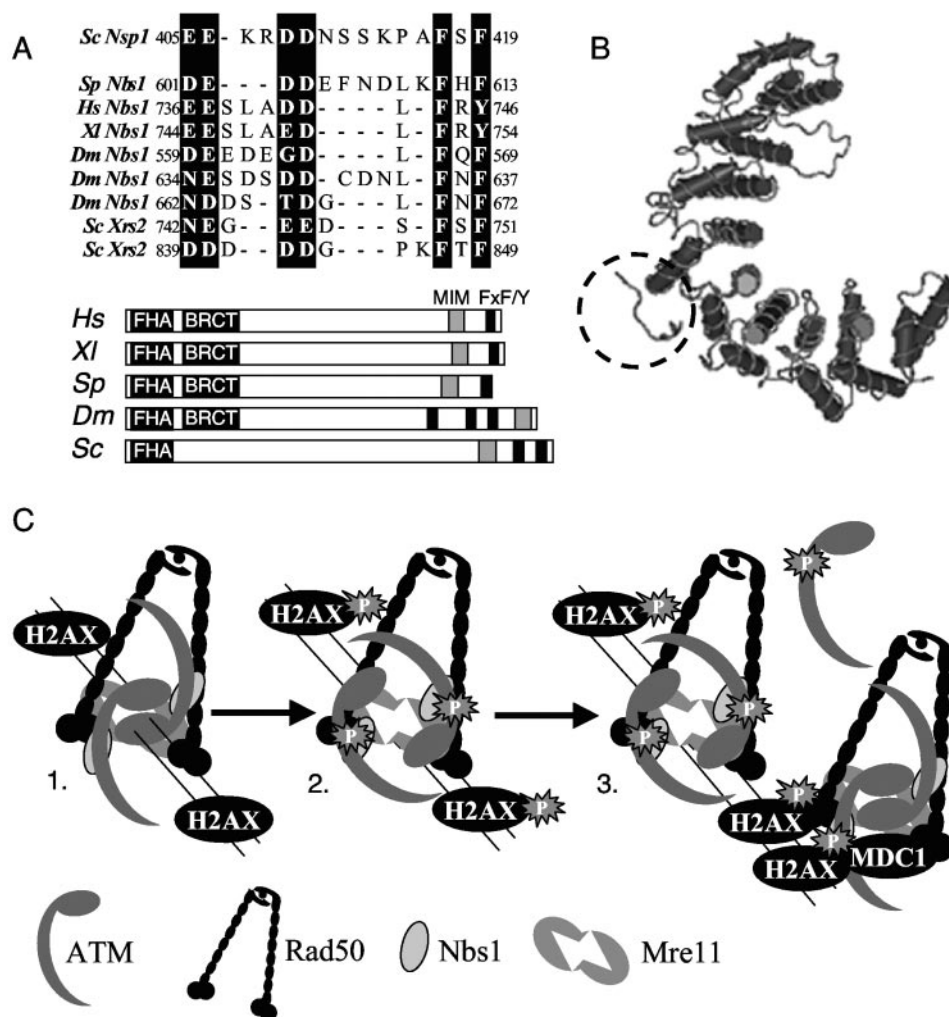


FIG. 8. Model of ATM activation. (A) Location of FxF/Y motifs preceded by the acidic patch in Nbs1 proteins from *Schizosaccharomyces pombe* (Sp), *Saccharomyces cerevisiae* (Sc), *Homo sapiens* (Hs), *Xenopus laevis* (Xl), and *Drosophila melanogaster* (Dm). The HEAT interaction region of *S. cerevisiae* nucleoporin Nsp1 is also shown. The lower panel shows a schematic representation of the Nbs1 proteins and the positions of FHA domains, BRCT domains, Mre11-interaction motif (MIM), and FxF/Y motifs. (B) Structure of an FxFG peptide interacting with HEAT repeats 5 and 6 of importin- β (6). (C) Proposed mechanism of ATM activation by DSBs. In step 1, the inactive ATM/MRN complex is recruited to sites of DNA damage. In step 2, ATP binding and hydrolysis induce conformational changes within the DNA-bound MRN/ATM complex that disengage the ATM dimer. ATM dimer disengagement leads to ATM autophosphorylation and phosphorylation of downstream effectors, such as H2AX. In step 3, the amplification of checkpoint signal by recruitment, activation, and release of ATM and by recruitment of additional MRN/ATM complexes via interactions with phospho-H2AX and MDC1 is shown. See the text for a more detailed description.

acidic patch and FxF motif at the extreme C terminus of Xrs2. We do not believe these findings invalidate our conclusions about the role of FxF/Y motifs in binding to Tel1/ATM. Instead, we hypothesize that Xrs2 has two Tel1-binding domains in its C-terminal 162 amino acids, only one of which aligns with the Tel1/ATM-binding domains at the extreme C terminus of Nbs1 proteins in fission yeast, *Xenopus*, and humans. Xrs2 has a second FxF motif preceded by acidic amino acids located ~100 amino acids from its C terminus (Fig. 8A). The 162-amino-acid C-terminal truncation of Xrs2, which removes both FxF motifs, abolishes the binding to Tel1 (50). In contrast to Xrs2, fission yeast and human Nbs1 have only one FxF/Y motif (Fig. 8A), which explains why point mutations in these motifs fully abrogate binding to Tel1/ATM. In Nbs1 proteins from some other organisms, there are no FxF/Y motifs in the

region C-terminal to the Mre11-binding motif. An example is the Nbs1 homolog in *Drosophila*, which instead has three FxF motifs located on the N-terminal side of the Mre11-binding motif. All of these FxF motifs are preceded by an acidic patch of amino acids (Fig. 8A). We hypothesize that these FxF/Y motifs define three separate ATM-binding sites in the *Drosophila* Nbs1 homolog.

The C terminus of Nbs1 engages specific HEAT repeats in Tel1. Two-hybrid analyses have shown that the C terminus of *S. pombe* Nbs1 interacts specifically with HEAT repeat pairs 17-18 and 21-22 in Tel1. Therefore, it is very likely that Tel1 has two separate Nbs1-binding domains. Importantly, the C-terminal 50 amino acids of Nbs1 were sufficient for this interaction, and it was abolished by point mutations in the FxF motif of full-length Nbs1. These findings suggest that Nbs1

makes specific contacts with binding pockets contained within HEAT repeats 17-18 and 21-22. A prediction of these studies is that the expression of these HEAT repeats alone may interfere with the interaction between endogenous Tel1 and Nbs1. We have not yet tested this prediction in fission yeast, but we note that overexpression of an ATM fragment encompassing HEAT repeats 14-25 causes a dominant negative effect in mammalian cells (12, 49). It prevents ATM activation, increases chromosome breakage and radiosensitivity, and impairs telomere maintenance. It will be interesting to determine whether these effects are caused by binding to endogenous Nbs1.

HEAT repeats are found in many classes of proteins (57). One well-studied example is importin- β , which consists entirely of 19 HEAT repeats (13, 14). Importin- β associates with importin- α , nucleoporins, and Ran-GTP, and together these proteins carry out nucleocytoplasmic trafficking of proteins and other macromolecules. Biochemical and mutational analyses showed that the interaction between importin- β and nucleoporins involves functionally redundant FXFG repeats in nucleoporins (63). These FXFG repeats are interspersed with hydrophilic patches of amino acids (63). The exact relevance of these hydrophilic patches is unknown, but they are an omnipresent feature among all FXFG-containing nucleoporins. Crystallographic analysis showed that an FXFG-containing peptide directly engages HEAT repeats 5 and 6 in importin- β (Fig. 8B) (6). The lining of the primary binding pocket for the two phenylalanines is constituted of hydrophobic residues from the A-helices of HEAT repeats 5 and 6. Interestingly, a secondary FXFG binding pocket is found in A-helices of HEAT repeats 6 and 7. The A-helices are on the convex side of the superhelical HEAT repeat structure (Fig. 8B) (6). By contrast, the binding sites for cargo and importin- α are on the concave side of the importin- β superhelical HEAT repeat structure (14). This configuration is ideal for the function of importin- β during nuclear transport (6).

In view of the crystallographic evidence that specific HEAT repeats in importin- β contain binding pockets for FXFG sequences in nucleoporins, it is striking that the FXF motif of *S. pombe* Nbs1 is essential for its interaction with specific HEAT repeats in Tel1. It is also striking that the FXF/Y motif in Nbs1 homologs is always preceded by an acidic patch of amino acids, similar to the hydrophilic patches of amino acids that separate FXFG motifs in nucleoporins. Our studies have shown that the acidic patch is essential for the interaction with Tel1/ATM.

Unlike the FXFG sequences in nucleoporins, the FXF/Y motif in Nbs1 homologs is not followed by a glycine residue. However, crystallographic studies suggest that the glycine residue does not make primary contacts with the A-helices (6). The glycine residue may serve as part of a spacer sequence. A spacer sequence would not be expected to be necessary at the extreme C terminus of Nbs1. Alternatively, the HEAT binding domains of Nbs1 and importin- β may have related but not identical specificities.

The evidence that multiple FXFG repeats in nucleoporins can interact with two separate but closely spaced HEAT repeats in importin- β is also interesting in light of our findings that the FXF motif in *S. pombe* Nbs1 can contact two separate but closely spaced HEAT repeats in Tel1. The structure of *S. cerevisiae* Xrs2 and *Drosophila* Nbs1, which we propose have

multiple FXF motifs that contact Tel1/ATM, also bears a resemblance to the existence of redundant FXFG motifs in nucleoporins. In view of all of these similarities, it is very tempting to propose that the C-terminal FXF/Y motif in Nbs1 contacts the convex face of a superhelical HEAT repeat domain in Tel1/ATM in a manner that closely resembles the interactions between nucleoporins and importin- β (Fig. 8B). Future structural analyses will be required to test this hypothesis.

Nbs1 is required for ATM activation in the *Xenopus* egg extract. It is evident from our studies in fission yeast and the previous analysis of budding yeast that the function of Tel1 is absolutely dependent on its ability to interact with Nbs1/Xrs2 (50). This relationship can be explained, at least in part, in the requirement for Xrs2 to recruit Tel1 to sites of DNA damage, where it can phosphorylate its targets (50). Indeed, these findings in yeast are fully consistent with evidence that active ATM is unable to form IR-induced foci in cells derived from NBS patients (38). A crucial question that cannot be conclusively addressed in yeast, or in cells from NBS patients, is whether Nbs1 is essential for Tel1/ATM activation. In yeasts, Tel1 is not known to autophosphorylate; therefore, it is not possible to discern whether Nbs1 is specifically required for Tel activation or is essential for recruitment of activated Tel1 to DSBs where it can phosphorylate its substrates. Almost all NBS patients have the same mutation, NBS1-657del5 (46). Cells from these patients are able to express an N-terminally truncated form of Nbs1, albeit at significantly reduced levels, and it is therefore impossible to know whether these cells are truly null for Nbs1 function (46). Indeed, recent studies of mouse embryonic fibroblasts containing an inducible null allele of NBS1 have shown that it is essential for cell viability (20). Therefore, it is highly unlikely that NBS patients, and the cells derived from those patients, could survive without the expression of a C-terminal portion of Nbs1 that includes the Mre11- and ATM-binding domains.

ATM autophosphorylation has been assayed in NBS cells, in cells in which Nbs1 protein abundance has been diminished by Nbs1 small interfering RNA, and in cells in which Mre11 degradation has been triggered by adenovirus infection (9, 10, 36, 38, 48, 73). In most experiments, ATM autophosphorylation was impaired but not eliminated, but in some exceptional cases there was no defect in ATM autophosphorylation. The exceptional situations involved exposure of NBS cells to moderate or high doses of ionizing radiation (38). These observations have suggested that the MRN complex is not required for ATM activation but is instead required to target activated ATM to sites of DNA damage (5). By this mechanism, the MRN complex has been proposed to contribute to ATM activation in response to small amounts of DNA damage by "sensing" the damage, amplifying the activation signal, or stabilizing the phosphorylated ATM (5). A conclusive test of this model has awaited the ability to fully eliminate Nbs1 function in a system in which ATM autophosphorylation can be monitored with phospho-S1981 antibodies. We therefore turned to the *Xenopus* egg extract system to address the question of whether Nbs1 is required for ATM activation in response to DNA damage. ATM undergoes S1981 autophosphorylation in response to damaged DNA in *Xenopus* egg extracts; thus, it is possible to directly assay ATM activation (65). Our studies

showed that antibodies specific to the C terminus of Nbs1 prevented S1981 phosphorylation in response to linear double-stranded DNA molecules, whose ends mimic DSBs in damaged DNA. Depletion of Nbs1 from the extract had the same effect. Importantly, virtually identical results were obtained by addition of *Xenopus* sperm chromatin cleaved with EcoRI endonuclease. Remarkably, a recombinant form of the Nbs1 C terminus that contained just the Mre11- and ATM-binding domains was able to restore ATM activation to an Nbs1-depleted extract. This fragment of Nbs1 also restored ATM recruitment to damaged DNA. These findings unequivocally demonstrate that in this experimental system Nbs1 is essential for ATM activation in response to damaged DNA.

It is important to note that about half of the Mre11 protein remained in the Nbs1-depleted extracts (Fig. 6B and F). We have not examined Rad50 in these extracts, but we presume that a substantial amount of it must have also remained in the Nbs1-depleted extract because ATM activation could be restored to the extract by addition of the recombinant form of the Nbs1 C terminus. The inability to more fully remove Mre11 by Nbs1 immunodepletion is somewhat surprising because gel filtration analysis of extracts from mammalian cells has suggested that most of the Mre11 is in a complex with Rad50 and Nbs1 (8). The situation may be different in *Xenopus* eggs. The *Xenopus* egg contains stockpiles of proteins needed for 12 subsequent divisions, and therefore, unlike somatic cells, the egg extract may contain separate pools of the Nbs1, Mre11, and Rad50 MRN subunits in addition to assembled MRN, which could account for the fact that complete depletion of Nbs1 does not result in complete depletion of Mre11 (or presumably of Rad50). It is also possible that some of the Nbs1 was stripped from the Mre11-Rad50 complex during the immunoprecipitation.

Studies carried out with purified proteins have shown that the Mre11-Rad50 complex can stimulate ATM activity toward p53 but not Chk2 (42). These findings suggested that the Mre11-Rad50 complex has some ability to interact with ATM in the absence of Nbs1. In contrast, studies in budding yeast (50), and our investigations of fission yeast cells and *Xenopus* egg extracts, have shown that a productive interaction between the MRN(X) complex and ATM/Tel1 in these systems is dependent on the C-terminal region of Nbs1. Perhaps the Mre11-Rad50 complex has a weak interaction with ATM that can be detected only with high concentrations of proteins in a purified system.

Our data support a model in which the recruitment of ATM to damaged DNA and its activation are coupled through an interaction with the C terminus of Nbs1. According to this model, the recruitment of ATM to damaged DNA should precede its activation. We have indeed observed this sequence of events in the *Xenopus* egg extract system. ATM that is unphosphorylated at S1981 can be detected bound to damaged DNA soon after the DNA is added to the extract. The same is true of damaged sperm chromatin. Indeed, we have observed ATM associated with Nbs1 without DNA added to the extract. Therefore, in contrast to the conclusions derived from studies of mammalian cells (4), we deduce from our experiments with the *Xenopus* egg extract that autophosphorylation of ATM is not a precondition for its association with Nbs1 or its recruitment to damaged DNA.

We have shown that Nbs1 is required for the S1981 phosphorylation of ATM that is induced by DSBs in the *Xenopus* egg extract. We have not addressed whether other forms of genotoxic stress can activate ATM in this system. In at least some types of mammalian cells, chloroquine and trichostatin A can induce S1981 phosphorylation of ATM without inducing phosphorylation of ATM substrates that are localized at sites of DNA damage (4, 38). Chloroquine is a topoisomerase II inhibitor and a DNA-intercalating agent. Trichostatin A is an inhibitor of histone deacetylases. Both of these agents are expected to increase torsional stress in DNA. Hypotonic buffers may have a similar effect. This torsional stress will generate secondary structures in DNA, such as hairpins, especially in palindromic sequences. The MRN complex is known to bind and process these structures (18, 24). Conceivably, the MRN complex will recruit ATM to these sites, and ATM will undergo autophosphorylation. However, these sites are expected to be devoid of histones and other DNA-bound proteins, such as SMC1, because torsionally stressed DNA will not adopt the B form conformation. Hence, these substrates may not be available to be phosphorylated by ATM. It is also possible that these DNA-bound proteins are necessary for the efficient retention of MRN and ATM at these sites. The efficient retention of the MRN complex requires MDC1, which is recruited to phospho-H2AX (45). Therefore, the large-scale recruitment and retention of MRN and ATM, and the subsequent phosphorylation of ATM substrates at sites of DNA damage, may not occur efficiently at sites of secondary structure in DNA. Upon binding to hairpins, the MRN complex will cleave the DNA to generate a nicked duplex that will relieve the torsional stress, leading to release of the MRN complex from the DNA. Conceivably, this transient association of MRN complex with DNA will induce ATM autophosphorylation but will not result in efficient phosphorylation of DNA-bound substrates.

Our findings coincide with a recent study by Falck et al., who found that the extreme C terminus of human Nbs1 is required for its association with ATM (23). On this point our findings are in agreement; however, our studies disagree on the functional significance of this interaction. Falck et al. found that a 20-amino-acid truncation at the C terminus of Nbs1 abolished its interaction with ATM but did not prevent it from fully complementing the partial defect in ATM autophosphorylation in NBS cells. However, this construct was unable to complement defects in phosphorylation of SMC1 or Chk2. These findings support a model in which ATM is activated in a mechanism that does not require a direct interaction with the MRN complex, although such an interaction is required for recruitment of ATM to sites of DNA damage (23). In contrast, our studies with the *Xenopus* egg extract have shown that the interaction of ATM with the C terminus of Nbs1 is absolutely essential for activation of ATM by DNA damage. Moreover, we have seen that recruitment of the unphosphorylated form of ATM to damaged DNA can precede ATM autophosphorylation.

It is unclear how to reconcile our data with the studies of Falck et al. (23). One possibility is that mammalian somatic cells and *Xenopus* eggs activate ATM by different mechanisms, although this explanation seems unlikely in view of previous evidence of highly conserved checkpoint mechanisms in the two experimental systems. A more likely explanation could

involve a mechanism of partial interallelic complementation of NBS cells. Numerous examples of interallelic complementation have been described for yeast and *Drosophila* (53, 59). These typically involve multimeric protein complexes in which the proteins have discrete functional domains. NBS cells express reduced levels of a ~70-kDa C-terminal fragment of Nbs1 that contains both the Mre11- and ATM-binding domains but lacks the forkhead-associated (FHA) and BRCA1 C-terminal (BRCT) domains (8). By expressing a C-terminal truncation of Nbs1 that lacks only the ATM-binding domain, it may be possible to form MRN complexes that contain both mutant forms of Nbs1. These complexes may be sufficient to fully restore ATM activation but unable to sustain efficient phosphorylation of ATM substrates. Another possibility involves the localization of Mre11 and Rad50. Most of the Mre11 and Rad50 in NBS cells is localized in the cytoplasm, presumably because Nbs1 is required for efficient localization of the MRN complex in the nucleus (8). Expression of Nbs1 that lacks only the ATM-binding region in NBS cells would be expected to fully complement the defect in nuclear localization of the MRN complex. This complex should be fully functional in all but one respect, the ability to interact with ATM. Perhaps by performing ATM-independent functions, the MRN complex that has the C-terminal truncation of Nbs1 will allow more of the MRN complexes that have the 70-kDa C-terminal fragment of Nbs1 to interact with ATM and bring about ATM activation in response to DNA damage.

A model of ATM activation in response to DNA damage.

Ataxia-telangiectasia, NBS, and ATLD patients share a number of symptomatic features, particularly a hypersensitivity to ionizing radiation (41, 66). These similarities have spurred speculation that the genes mutated in these patients participate in a common pathway of DNA damage response. With the identification of the genes mutated in these patients, and the realization that ATM, Nbs1, and Mre11 have well-characterized functional homologs in yeasts and other experimental organisms, there has been an increasing realization that ATM and the MRN complex have closely intertwined functions. Our studies have provided new mechanistic insights into the way in which these proteins interact and their functional relevance. We have unearthed evidence that specific HEAT repeats in *S. pombe* Tel1 mediate the physical interaction with Nbs1 and have found that this interaction bears a striking resemblance to the structurally characterized interaction between nucleoporins and importin- β . We have also found that the autophosphorylation of ATM and its recruitment to damaged DNA are functionally linked through the interaction with the C terminus of Nbs1.

Structural studies of the MRN complex, coupled with biochemical analyses, have indicated that the complex acts as a macromolecular machine that hydrolyzes ATP as an energy source (34). As is the case for most ATP-consuming macromolecular machines, ATP binding and hydrolysis induce major conformational changes that are critical for the function of these machines. For example, ATP binding and hydrolysis induce conformational changes in ABC transporters that are critical for their function in transmembrane efflux (35). Similarly, the mechanism of protein folding in the bacterial GroEL/ES machine is governed by successive steps of ATP binding and hydrolysis that induce critical conformational

changes in the complex (68). In budding yeast, the subunits of the Mre11-Rad50-Xrs2 complex are the first proteins that can be detected at a DSB, consistent with the idea that this complex is the initial sensor of damaged DNA (44). Upon binding of the MRN complex to damaged DNA, ATP binding and hydrolysis by Rad50 induce conformational changes in the complex (34). Given these facts, and the evidence that Rad50 and Mre11 homologs exist in bacteria and presumably predate the appearance of Nbs1 and ATM during evolution (33), it is reasonable to propose that Nbs1 and ATM have coevolved to be able to use conformational changes in the MRN complex to sense DNA damage (Fig. 8C). Our findings that *S. pombe* Tel1 and Nbs1 can be coprecipitated from cells in the absence of DNA damage, and that *Xenopus* ATM coprecipitates with Nbs1 without addition of DNA to the extract, and previous studies that have shown budding yeast Tel1 coprecipitates with Xrs2 prior to DNA damage (50) suggest that at least a subpopulation of MRN and Tel1/ATM molecules exist as a pre-assembled complex prior to DNA damage. It is reasonable to propose that upon DNA damage, these preassembled complexes will quickly relocate to sites of DNA damage (Fig. 8C). Following interaction with DNA, ATP-induced conformational changes in Rad50 will be propagated through Mre11 and Nbs1 to ATM, leading to a conformational change in ATM that results in its activation (Fig. 7C). Given evidence in mammalian cells that ATM exists as inactive multimers in large protein complexes (4), we propose that the conformational change in the MRN complex disengages ATM multimers and relieves autoinhibition, leading to ATM activation and autophosphorylation (Fig. 8C). In this mechanism, the activation of ATM is strictly coupled to the interaction of the MRN complex with damaged DNA, thereby ensuring that ATM is maintained in an inhibited state in the absence of DNA damage.

In LB-1 cells derived from NBS patients, which can express a truncated form of Nbs1 that lacks the N-terminal FHA and BRCT domains (46), it is possible to achieve robust activation of ATM at higher doses of IR, and yet ATM substrates, such as SMC1 and Chk2, are inefficiently phosphorylated (4, 38). Based on our model, one could propose that ATM activation is not ablated in LB-1 cells, because the large C-terminal fragment of Nbs1 that is expressed in these cells can recruit ATM to damaged DNA and trigger its activation. However, the association of ATM with downstream target proteins is defective because this association is dependent on the FHA and BRCT domains of Nbs1. LB-1 cells have diminished ATM activation at low doses of IR (4, 36). Again, this defect might be attributed to the absence of the FHA and BRCT domains in the truncated form of Nbs1 that is expressed in these cells. These domains might play a critical role in the retention of the complex at sites of DNA damage through interactions with phospho-H2AX and/or MDC1 (39, 45). If retention and accumulation of the MRN complex at sites of DNA damage are required for amplification of the checkpoint signal, perhaps through spreading of the MRN complex to regions of DNA adjacent to a DSB (Fig. 8C), then diminished activation of ATM at low doses of IR might be an expected consequence of mutations that truncate the FHA and BRCT domains. A positive feedback loop in which phospho-H2A recruits MDC1, which in turn recruits more MRN complex that associates with ATM, could easily explain how as few as 18 DSBs, which are

estimated to be caused by irradiation of diploid human cells with 0.5 Gy of IR, can activate over 50% of the total cellular pool of ATM (4). Extensive activation of ATM by a small number of DSBs might also be explained by a mechanism in which there is continuous recruitment, activation, and release of ATM by the MRN complexes near DSBs (Fig. 8C). The release rate of activated ATM could be affected by the phosphorylation of ATM itself and by phosphorylation of ATM substrates. Higher doses of IR will cause more DSBs and lead to recruitment of MRN and ATM at more sites in the genome, resulting in increased phosphorylation of ATM substrates that are bound to DNA, such as H2AX and SMC1.

Regulation of ATR and other PIKKs. The evidence that ATM/Tel1 homologs interact with the C terminus of Nbs1 may have implications for the regulation and function of other members of the PIKK family. ATR and its homologs in fission and budding yeast interact with regulatory subunits that are known as ATRIP, Rad26, and Ddc2/Lcd1/Pie1, respectively (62). Interestingly, a truncation of the C-terminal 30 amino acids from Ddc2 abolishes its interaction with Mec1 in budding yeast (74). It is known that the C-terminal 30 amino acids of Rad26 are essential for the checkpoint function of the Rad3-Rad26 complex (43). It is tempting to speculate that the C terminus of Ddc2 has a motif that interacts with one or more HEAT repeats in Mec1. The C termini of the ATRIP/Rad26/Ddc2 family of proteins do not possess FxF/Y-like motifs, but the interaction between this family of proteins and ATR homologs could involve a distinct mode of HEAT repeat interaction. Active DNA-PK consists of the catalytic subunit DNA-PKcs, which is a PIKK that contains a large N-terminal HEAT repeat domain, and a Ku70-Ku80 heterodimer (69). DNA-PKcs interacts with the C-terminal domain of Ku80 (26). A recent structural study of the Ku80 C-terminal domain showed that it shares structural similarity to a helical HEAT-like repeat in RabGGT α (76). Interestingly, this region of RabGGT α is required for an interhelical interaction with RabGGT β . It is therefore possible that the binding of Ku80 and DNA-PKcs is an analogous inter-HEAT repeats interaction. Thus, while the interactions between PIKKs and their regulatory subunits seem to involve the C-terminal ends of the regulatory molecules, the modes of interaction might involve distinct structural modules that interact with HEAT repeats.

ACKNOWLEDGMENTS

We thank Li-Lin Du, Martin Hetzer, Gerard Manning, John Newport, John Tainer, and Matthew Weitzman for reagents, discussions, and technical support.

T.H. is a Frank and Else Schilling American Cancer Society Research Professor. This work was funded by NCI grant CA80100, awarded to T.H., and grants GM59447 and CA77325, awarded to P.R.

REFERENCES

1. Abraham, R. T. 2001. Cell cycle checkpoint signaling through the ATM and ATR kinases. *Genes Dev.* **15**:2177–2196.
2. Andrade, M. A., C. Petosa, S. I. O'Donoghue, C. W. Muller, and P. Bork. 2001. Comparison of ARM and HEAT protein repeats. *J. Mol. Biol.* **309**: 1–18.
3. Bahler, J., J. Q. Wu, M. S. Longtine, N. G. Shah, A. McKenzie III, A. B. Steever, A. Wach, P. Philippsen, and J. R. Pringle. 1998. Heterologous modules for efficient and versatile PCR-based gene targeting in *Schizosaccharomyces pombe*. *Yeast* **14**:943–951.
4. Bakkenist, C. J., and M. B. Kastan. 2003. DNA damage activates ATM through intermolecular autophosphorylation and dimer dissociation. *Nature* **421**:499–506.
5. Bakkenist, C. J., and M. B. Kastan. 2004. Initiating cellular stress responses. *Cell* **118**:9–17.
6. Bayliss, R., T. Littlewood, and M. Stewart. 2000. Structural basis for the interaction between FxFG nucleoporin repeats and importin-beta in nuclear trafficking. *Cell* **102**:99–108.
7. Blow, J. J., and R. A. Laskey. 1986. Initiation of DNA replication in nuclei and purified DNA by a cell-free extract of *Xenopus* eggs. *Cell* **47**:577–587.
8. Carney, J. P., R. S. Maser, H. Olivares, E. M. Davis, M. Le Beau, J. R. Yates III, L. Hays, W. F. Morgan, and J. H. Petrini. 1998. The hMre11/hRad50 protein complex and Nijmegen breakage syndrome: linkage of double-strand break repair to the cellular DNA damage response. *Cell* **93**:477–486.
9. Carson, C. T., R. A. Schwartz, T. H. Stracker, C. E. Lilley, D. V. Lee, and M. D. Weitzman. 2003. The Mre11 complex is required for ATM activation and the G2/M checkpoint. *EMBO J.* **22**:6610–6620.
10. Cerosaletti, K., and P. Concannon. 2004. Independent roles for nibrin and Mre11/Rad50 in the activation and function of Atm. *J. Biol. Chem.* **279**: 38813–38819.
11. Chahwan, C., T. M. Nakamura, S. Sivakumar, P. Russell, and N. Rhind. 2003. The fission yeast Rad32 (Mre11)-Rad50-Nbs1 complex is required for the S-phase DNA damage checkpoint. *Mol. Cell. Biol.* **23**:6564–6573.
12. Chen, S., P. Paul, and B. D. Price. 2003. ATM's leucine-rich domain and adjacent sequences are essential for ATM to regulate the DNA damage response. *Oncogene* **22**:6332–6339.
13. Chook, Y. M., and G. Blobel. 1999. Structure of the nuclear transport complex karyopherin-beta2-Ran x GppNHp. *Nature* **399**:230–237.
14. Cingolani, G., C. Petosa, K. Weis, and C. W. Muller. 1999. Structure of importin-beta bound to the IBB domain of importin-alpha. *Nature* **399**:221–229.
15. Connelly, J. C., and D. R. Leach. 2002. Tethering on the brink: the evolutionarily conserved Mre11-Rad50 complex. *Trends Biochem. Sci.* **27**:410–418.
16. Costanzo, V., T. Paull, M. Gottesman, and J. Gautier. 2004. Mre11 assembles linear DNA fragments into DNA damage signaling complexes. *PLoS Biol.* **2**:600–609.
17. Costanzo, V., K. Robertson, C. Y. Ying, E. Kim, E. Avvedimento, M. Gottesman, D. Grieco, and J. Gautier. 2000. Reconstitution of an ATM-dependent checkpoint that inhibits chromosomal DNA replication following DNA damage. *Mol. Cell* **6**:649–659.
18. D'Amours, D., and S. P. Jackson. 2002. The Mre11 complex: at the crossroads of DNA repair and checkpoint signaling. *Nat. Rev. Mol. Cell Biol.* **3**:317–327.
19. Delia, D., M. Piane, G. Buscemi, C. Savio, S. Palmeri, P. Lulli, L. Carlessi, E. Fontanella, and L. Chessa. 2004. MRE11 mutations and impaired ATM-dependent responses in an Italian family with ataxia-telangiectasia-like disorder. *Hum. Mol. Genet.* **13**:2155–2163.
20. Demuth, L., P. O. Frappart, G. Hildebrand, A. Melchers, S. Lobitz, L. Stockl, R. Varon, Z. Herceg, K. Sperling, Z. Q. Wang, and M. Digweed. 2004. An inducible null mutant murine model of Nijmegen breakage syndrome proves the essential function of NBS1 in chromosomal stability and cell viability. *Hum. Mol. Genet.* **13**:2385–2397.
21. Desai-Mehta, A., K. M. Cerosaletti, and P. Concannon. 2001. Distinct functional domains of nibrin mediate Mre11 binding, focus formation, and nuclear localization. *Mol. Cell. Biol.* **21**:2184–2191.
22. Du, L. L., T. M. Nakamura, B. A. Moser, and P. Russell. 2003. Retention but not recruitment of Crb2 at double-strand breaks requires Rad1 and Rad3 complexes. *Mol. Cell. Biol.* **23**:6150–6158.
23. Falck, J., J. Coates, and S. P. Jackson. 2005. Conserved modes of recruitment of ATM, ATR and DNA-PKcs to sites of DNA damage. *Nature* **434**:605–611.
24. Farah, J. A., E. Hartsuiker, K. Mizuno, K. Ohta, and G. R. Smith. 2002. A 160-bp palindrome is a Rad50. Rad32-dependent mitotic recombination hotspot in *Schizosaccharomyces pombe*. *Genetics* **161**:461–468.
25. Fernandez-Capetillo, O., A. Lee, M. Nussenzweig, and A. Nussenzweig. 2004. H2AX: the histone guardian of the genome. *DNA Repair (Amsterdam)* **3**:959–967.
26. Gell, D., and S. P. Jackson. 1999. Mapping of protein-protein interactions within the DNA-dependent protein kinase complex. *Nucleic Acids Res.* **27**:3494–3502.
27. Gottesfeld, J., and L. S. Bloomer. 1982. Assembly of transcriptionally active 5S RNA gene chromatin in vitro. *Cell* **28**:781–791.
28. Groves, M. R., N. Hanlon, P. Turowski, B. A. Hemmings, and D. Barford. 1999. The structure of the protein phosphatase 2A PR65/A subunit reveals the conformation of its 15 tandemly repeated HEAT motifs. *Cell* **96**:99–110.
29. Guo, Z., and W. G. Dunphy. 2000. Response of *Xenopus* Cds1 in cell-free extracts to DNA templates with double-stranded ends. *Mol. Biol. Cell* **11**: 1535–1546.
30. Haber, J. E. 1998. The many interfaces of Mre11. *Cell* **95**:583–586.
31. Heckman, D. S., D. M. Geiser, B. R. Eidell, R. L. Stauffer, N. L. Kardos, and S. B. Hedges. 2001. Molecular evidence for the early colonization of land by fungi and plants. *Science* **293**:1129–1133.
32. Hodson, J. A., J. M. Bailis, and S. L. Forsburg. 2003. Efficient labeling of

- fission yeast *Schizosaccharomyces pombe* with thymidine and BUdR. *Nucleic Acids Res.* **31**:e134.
33. Hopfner, K. P., A. Karcher, D. Shin, C. Fairley, J. A. Tainer, and J. P. Carney. 2000. Mre11 and Rad50 from *Pyrococcus furiosus*: cloning and biochemical characterization reveal an evolutionarily conserved multiprotein machine. *J. Bacteriol.* **182**:6036–6041.
 34. Hopfner, K. P., A. Karcher, D. S. Shin, L. Craig, L. M. Arthur, J. P. Carney, and J. A. Tainer. 2000. Structural biology of Rad50 ATPase: ATP-driven conformational control in DNA double-strand break repair and the ABC-ATPase superfamily. *Cell* **101**:789–800.
 35. Hopfner, K. P., and J. A. Tainer. 2003. Rad50/SMC proteins and ABC transporters: unifying concepts from high-resolution structures. *Curr. Opin. Struct. Biol.* **13**:249–255.
 36. Horejsi, Z., J. Falck, C. J. Bakkenist, M. B. Kastan, J. Lukas, and J. Bartek. 2004. Distinct functional domains of Nbs1 modulate the timing and magnitude of ATM activation after low doses of ionizing radiation. *Oncogene* **23**:3122–3127.
 37. Kastan, M. B., and J. Bartek. 2004. Cell-cycle checkpoints and cancer. *Nature* **432**:316–323.
 38. Kitagawa, R., C. J. Bakkenist, P. J. McKinnon, and M. B. Kastan. 2004. Phosphorylation of SMC1 is a critical downstream event in the ATM-NBS1-*BRCA1* pathway. *Genes Dev.* **18**:1423–1438.
 39. Kobayashi, J., H. Tauchi, S. Sakamoto, A. Nakamura, K. Morishima, S. Matsuura, T. Kobayashi, K. Tamai, K. Tanimoto, and K. Komatsu. 2002. NBS1 localizes to gamma-H2AX foci through interaction with the FHA/BRCT domain. *Curr. Biol.* **12**:1846–1851.
 40. Laskey, R. A., and W. C. Earnshaw. 1980. Nucleosome assembly. *Nature* **286**:763–767.
 41. Lavin, M. F., and Y. Shiloh. 1997. The genetic defect in ataxia-telangiectasia. *Annu. Rev. Immunol.* **15**:177–202.
 42. Lee, J. H., and T. T. Paull. 2004. Direct activation of the ATM protein kinase by the Mre11/Rad50/Nbs1 complex. *Science* **304**:93–96.
 43. Lindsay, H. D., D. J. Griffiths, R. J. Edwards, P. U. Christensen, J. M. Murray, F. Osman, N. Walworth, and A. M. Carr. 1998. S-phase-specific activation of Cds1 kinase defines a subpathway of the checkpoint response in *Schizosaccharomyces pombe*. *Genes Dev.* **12**:382–395.
 44. Lisby, M., J. H. Barlow, R. C. Burgess, and R. Rothstein. 2004. Choreography of the DNA damage response: spatiotemporal relationships among checkpoint and repair proteins. *Cell* **118**:699–713.
 45. Lukas, C., F. Melander, M. Stucki, J. Falck, S. Bekker-Jensen, M. Goldberg, Y. Lereenthal, S. P. Jackson, J. Bartek, and J. Lukas. 2004. Mdc1 couples DNA double-strand break recognition by Nbs1 with its H2AX-dependent chromatin retention. *EMBO J.* **23**:2674–2683.
 46. Maser, R. S., R. Zinkel, and J. H. Petrini. 2001. An alternative mode of translation permits production of a variant NBS1 protein from the common Nijmegen breakage syndrome allele. *Nat. Genet.* **27**:417–421.
 47. Matsuura, A., T. Naito, and F. Ishikawa. 1999. Genetic control of telomere integrity in *Schizosaccharomyces pombe*: rad3⁺ and tel1⁺ are parts of two regulatory networks independent of the downstream protein kinases chk1⁺ and cds1⁺. *Genetics* **152**:1501–1512.
 48. Mochan, T. A., M. Venere, R. A. DiTullio, Jr., and T. D. Halazonetis. 2003. 53BP1 and NFB1/MDC1-Nbs1 function in parallel interacting pathways activating ataxia-telangiectasia mutated (ATM) in response to DNA damage. *Cancer Res.* **63**:8586–8591.
 49. Morgan, S. E., C. Lovly, T. K. Pandita, Y. Shiloh, and M. B. Kastan. 1997. Fragments of ATM which have dominant-negative or complementing activity. *Mol. Cell Biol.* **17**:2020–2029.
 50. Nakada, D., K. Matsumoto, and K. Sugimoto. 2003. ATM-related Tel1 associates with double-strand breaks through an Xrs2-dependent mechanism. *Genes Dev.* **17**:1957–1962.
 51. Nakamura, T. M., L. L. Du, C. Redon, and P. Russell. 2004. Histone H2A phosphorylation controls Crb2 recruitment at DNA breaks, maintains checkpoint arrest, and influences DNA repair in fission yeast. *Mol. Cell Biol.* **24**:6215–6230.
 52. Nakamura, T. M., B. A. Moser, and P. Russell. 2002. Telomere binding of checkpoint sensor and DNA repair proteins contributes to maintenance of functional fission yeast telomeres. *Genetics* **161**:1437–1452.
 53. Navas, T. A., Z. Zhou, and S. J. Elledge. 1995. DNA polymerase epsilon links the DNA replication machinery to the S phase checkpoint. *Cell* **80**:29–39.
 54. Newport, J. 1987. Nuclear reconstitution in vitro: stages of assembly around protein-free DNA. *Cell* **48**:205–217.
 55. Nyberg, K. A., R. J. Michelson, C. W. Putnam, and T. A. Weinert. 2002. Toward maintaining the genome: DNA damage and replication checkpoints. *Annu. Rev. Genet.* **36**:617–656.
 56. O'Driscoll, M., V. L. Ruiz-Perez, C. G. Woods, P. A. Jeggo, and J. A. Goodship. 2003. A splicing mutation affecting expression of ataxia-telangiectasia and Rad3-related protein (ATR) results in Seckel syndrome. *Nat. Genet.* **33**:497–501.
 57. Perry, J., and N. Kleckner. 2003. The ATRs, ATMs, and TORs are giant HEAT repeat proteins. *Cell* **112**:151–155.
 58. Petrini, J. H., and T. H. Stracker. 2003. The cellular response to DNA double-strand breaks: defining the sensors and mediators. *Trends Cell Biol.* **13**:458–462.
 59. Rawls, J. M., and J. W. Fristrom. 1975. A complex genetic locus that controls of the first three steps of pyrimidine biosynthesis in *Drosophila*. *Nature* **255**:738–740.
 60. Redon, C., D. Pilch, E. Rogakou, O. Sedelnikova, K. Newrock, and W. Bonner. 2002. Histone H2A variants H2AX and H2AZ. *Curr. Opin. Genet. Dev.* **12**:162–169.
 61. Ritchie, K. B., and T. D. Petes. 2000. The Mre11p/Rad50p/Xrs2p complex and the Tel1p function in a single pathway for telomere maintenance in yeast. *Genetics* **155**:475–479.
 62. Rouse, J., and S. P. Jackson. 2002. Interfaces between the detection, signaling, and repair of DNA damage. *Science* **297**:547–551.
 63. Rout, M. P., and S. R. Wentz. 1994. Pores for thought: nuclear pore complex proteins. *Trends Cell Biol.* **4**:357–365.
 64. Sanders, S. L., M. Portoso, J. Mata, J. Bahler, R. C. Allshire, and T. Kouzarides. 2004. Methylation of histone H4 lysine 20 controls recruitment of Crb2 to sites of DNA damage. *Cell* **119**:603–614.
 65. Shechter, D., V. Costanzo, and J. Gautier. 2004. ATR and ATM regulate the timing of DNA replication origin firing. *Nat. Cell Biol.* **6**:648–655.
 66. Shiloh, Y. 1997. Ataxia-telangiectasia and the Nijmegen breakage syndrome: related disorders but genes apart. *Annu. Rev. Genet.* **31**:635–662.
 67. Shiloh, Y. 2003. ATM and related protein kinases: safeguarding genome integrity. *Nat. Rev. Cancer* **3**:155–168.
 68. Sigler, P. B., Z. Xu, H. S. Rye, S. G. Burston, W. A. Fenton, and A. L. Horwich. 1998. Structure and function in GroEL-mediated protein folding. *Annu. Rev. Biochem.* **67**:581–608.
 69. Smith, G. C., and S. P. Jackson. 1999. The DNA-dependent protein kinase. *Genes Dev.* **13**:916–934.
 70. Tauchi, H., J. Kobayashi, K. Morishima, S. Matsuura, A. Nakamura, T. Shiraiishi, E. Ito, D. Masnada, D. Delia, and K. Komatsu. 2001. The fork-head-associated domain of NBS1 is essential for nuclear foci formation after irradiation but not essential for hRAD50-hMRE11-NBS1 complex DNA repair activity. *J. Biol. Chem.* **276**:12–15.
 71. Tsukamoto, Y., C. Mitsuoka, M. Terasawa, H. Ogawa, and T. Ogawa. 2005. Xrs2p regulates mre11p translocation to the nucleus and plays a role in telomere elongation and meiotic recombination. *Mol. Biol. Cell* **16**:597–608.
 72. Ueno, M., T. Nakazaki, Y. Akamatsu, K. Watanabe, K. Tomita, H. D. Lindsay, H. Shinagawa, and H. Iwasaki. 2003. Molecular characterization of the *Schizosaccharomyces pombe* nbs1⁺ gene involved in DNA repair and telomere maintenance. *Mol. Cell Biol.* **23**:6553–6563.
 73. Uziel, T., Y. Lereenthal, L. Moyal, Y. Andegeko, L. Mittelman, and Y. Shiloh. 2003. Requirement of the MRN complex for ATM activation by DNA damage. *EMBO J.* **22**:5612–5621.
 74. Wakayama, T., T. Kondo, S. Ando, K. Matsumoto, and K. Sugimoto. 2001. Pie1, a protein interacting with Mec1, controls cell growth and checkpoint responses in *Saccharomyces cerevisiae*. *Mol. Cell Biol.* **21**:755–764.
 75. You, Z., K. Harvey, L. Kong, and J. Newport. 2002. Xic1 degradation in *Xenopus* egg extracts is coupled to initiation of DNA replication. *Genes Dev.* **16**:1182–1194.
 76. Zhang, Z., W. Hu, L. Cano, T. D. Lee, D. J. Chen, and Y. Chen. 2004. Solution structure of the C-terminal domain of Ku80 suggests important sites for protein-protein interactions. *Structure (Cambridge)* **12**:495–502.